DEFENCE **R&D** DÉFENSE

New Stepped Frequency Waveform Algorithms for High Range Resolution Radar: Short Pulse Reconstruction and Short Pulse Identification

Edwin S. Riseborough
Defence Research Establishment Ottawa

Anna Wilkinson
xwave solutions

DEFENCE RESEARCH ESTABLISHMENT OTTAWA

National Défense
Defence nationale

Canadä

DEFENCE **RꞮꝹ** DÉFENSE

New Stepped Frequency Waveform Algorithms for High Range Resolution Radar: Short Pulse Reconstruction and Short Pulse Identification

Edwin S. Riseborough
Maritime Radar Group
Surface Radar Section

Anna Wilkinson
xwave solutions

DEFENCE RESEARCH ESTABLISHMENT OTTAWA

Abstract

One of the problems facing Multi-Function Radar (MFR) designers is a limited time budget. Since an MFR has to perform many functions in parallel, time consuming functions, such as high range resolution radar (HRR), face time constraints which gravely limit their capability. MFR's under development are planning to use the stepped frequency waveform to implement HRR since it is a relatively simple waveform to implement, however, this requires the radar to dwell on the target for a long time. This report describes two new relatively simple techniques, called the short pulse reconstruction (SPR) technique and the short pulse identification (SPI) technique, which can be used to reduce the dwell time required for HRR. The new techniques presented here use a smaller pulse width to sample portions of the target, and would make use of high-speed analog-to-digital data acquisition systems that should already be part of an MFR. The SPR technique can create the complete target high range resolution amplitude versus range profile (or HRR image) based on returns from overlapping HRR images. The SPI technique is also presented, which performs identification directly using adjacent HRR returns. Simulated studies for the SPR and SPI routines gave promising results. If the compensation is perfect then the SPR and SPI routines perform as well as the conventional HRR process. Inaccuracies in estimating the compensation requirements resulted in quite distorted HRR images. The identifiers only made use of the imperfect signatures, thus causing degradation in performance. However, the conventional HRR approach did not perform as well for most compensation errors. Since, at most, only half the frequencies are required by the SPR and SPI algorithms as that of the conventional HRR, the techniques are more sensitive to SNR. The SPR sorting routine was able to determine the geometry and relative signal strengths of various experimental configurations using an Experimental Array Radar System. While it is possible to reduce radar dwell times by implementing the SPR or SPI processes, the algorithms could also be used to enhance existing HRR systems by at least doubling the size of target they could identify.

Résumé

Un des problèmes rencontré par les concepteurs de radar multifonctions (RMF) est un budget limité en temps. Puisque qu'un RMF doit effectué plusieurs fonctions en parallèles, des fonctions qui prennent beaucoup de temps, comme la haute résolution en portée (HRP) d'un radar, font face à de graves contrainte temporelles affectant leurs performances. Les RMF en développement utiliserons une modulation discrète en fréquence pour obtenir la HRP puisque cela est une forme d'onde relativement facile a produire due à sa bande de fréquence étroite. Cependant cette forme d'onde produit un temps plus long d'illumination sur la cible. Ce rapport décrit deux nouvelles techniques relativement simples, appelée la technique de reconstruction à impulsions courtes (RIC) et la technique d'identification à impulsions courtes (IIC) lesquelles peuvent être utilisées pour réduire le temps d'illumination requis pour la HRP. Ces nouvelles techniques utilisent des impulsions de durée plus courtes pour échantillonner la cible. Ils utilisent aussi un système d'acquisition de données analogique - numérique haute vitesse qui sera déjà installée dans les RMF. La technique de reconstruction à impulsions courtes (RIC) peut reproduire l'amplitude en portée de toute la cible (image HRP) à partir des échos HRP qui se chevauchent. La technique IIC est aussi présentée, laquelle effectue directement l'identification de la cible à partir des images adjacentes HRP. Des études en simulations des techniques RIC et IIC ont données des résultats prometteurs. Si les compensations de mouvement sont exactes alors les routines RIC et IIC fonctionnent aussi bien que les techniques conventionnelles HRP. Des estimations imprécises sur les compensations de mouvement résultent en des images HRP très déformées. Les systèmes d'identification réelle utilisent seulement des signatures imparfaites, ceci causant une dégradation de leurs performances. Cependant, l'approche conventionnelle d'identification HRP ne fonctionne pas aussi bien en présence d'erreurs de compensation de mouvement. Les algorithmes de RIC et IIC sont plus sensible au SNR puisque qu'au plus seulement la moitié des fréquences discrètes sont nécessaires comparativement aux techniques conventionnelles de HRP. La routine de triage RIC est capable de déterminer la géométrie et l'amplitude des signaux pour différentes configurations expérimentales utilisant le radar à réseau expérimental. Les techniques RIC et IIC peuvent être utiliser pour réduire le temps d'illumination, aussi bien que pour améliorer les systèmes existant de HRP en doublant la grandeur des cibles qui peuvent être identifier.

Executive Summary

One of the problems facing Multi-Function Radar (MFR) designers is a limited time budget. An MFR has to perform many functions in parallel, such as horizon search, target engagement, clutter mapping and time-consuming functions, such as high range resolution radar (HRR). As HRR would be considered as a growth items for MFR's presently under development, the designers have to define the waveforms required by the HRR and include this capability in the MFR when it is built. This simplifies the installation of the HRR feature when it is ready. To do this involves selecting the maximum target size that the HRR system could identify, and the waveform to perform this task. Two waveforms can be used to achieve high range resolution, the pulse compression and stepped frequency waveforms. Pulse compression has the ability to acquire the HRR signature in one pulse. This requires a long transmitted pulse, of duration of hundreds of microseconds, and a matched filter receiver to extract the range profile. An MFR has many other functions to perform which don't require such a long pulse, to add pulse compression with very wide bandwidth (in the order of hundreds of Megahertz) adds complexity to the design, and using a waveform which doesn't require modification to the hardware is preferred. MFR's under development are planning to use the stepped frequency waveform to implement HRR since it is a relatively simple waveform to implement because of its use of narrow bandwidth pulses. Basically, the waveform consists of a train of pulses that step across a wide frequency band. The pulses are then integrated via an inverse FFT to get a high range resolution amplitude profile, or HRR image, of the target. An essential requirement of the stepped frequency method is that the transmitted pulses be wide enough to encompass the target being interrogated. This poses a problem in larger targets since the radar would have to transmit a longer pulse, then the frequency step size in the stepped frequency waveform would have to be reduced. This results in a long dwell time for the radar. Selecting the maximum target size that can be identified in an MFR using the stepped frequency waveform involves a complicated decision process.

This report describes two relatively simple techniques, called the short pulse reconstruction technique and the short pulse identification technique, which can be used to get the most out of the limited time budget that an MFR could schedule for performing HRR. The new techniques presented here use a smaller pulse width to sample portions of the target, and make use of high-speed analog-to-digital data acquisition systems that should already be part of the MFR. The Short Pulse Reconstruction (SPR) technique would create the complete target image based on adjacent overlapping HRR images. The SPR technique requires a routine for sorting the peak scatterers from the adjacent images. By using reduced pulse widths, the stepped frequency waveform would not require the smaller frequency step size; therefore, the radar dwell time is also reduced. Another possible advantage of the technique is that since the radar dwell time is reduced by at least half, this should reduce the motion compensation related distortions as well. An alternative approach to the SPR technique is also presented, which would attempt to perform identification on a target without reconstructing the target. The approach is called short pulse identification (SPI).

This report describes the SPR and SPI techniques, as well as the performance analysis involving motion compensation, and signal to noise ratio effects. Identification performance is studied using a process is similar to the sum of the moduli of normalized residuals (MNR). Experimental validation of the SPR process is presented using various configurations of corner reflectors.

Simulation studies involved the creation of a database of 100 randomly generated, but similar images at 11 aspect angles. A comparison was made between the SPR, SPI processes and the conventional HRR process and a low resolution version of the conventional HRR process was made. Only specific compensation errors (i.e. velocity compensation alone) were tried for each test to isolate the effect of each of the areas studied. Simulated studies for the SPR and SPI routines gave promising results. Inaccuracies in estimating the compensation requirements result in quite distorted HRR images. The identifiers only made use of the imperfect signatures, thus causing degradation in performance. Velocity and acceleration tolerant waveforms can be used to solve some of the compensation problems. If the compensation is perfect then the SPR and SPI routines perform as well as the conventional HRR process. They are more sensitive to SNR, but that is expected due to only half the number of points being integrated as compared to the conventional HRR process. The low resolution HRR performed better than all the other identifiers. This result highlights the problem of defining resolution requirements for HRR identification. The library generated for this study had targets containing up to 16 scatterers spread randomly across a 50 meter range. With this library, the identifiers may not need the 0.3 m resolution that the 500 MHz bandwidth gives to perform successfully. While the low resolution HRR approach worked better for this simulation, the SPR routine has demonstrated that it can be used to rebuild a target from multiple images, and also give good identification results. Determining a proper threshold is essential to the success of the SPR and SPI routines. Setting the threshold too low would let noise or compensation error induced peaks corrupt the final SPR images, or reduce the SPI process effectiveness for performing proper identification.

The SPR sorting routine was able to determine the geometry and relative signal strengths of various experimental configurations using an Experimental Array Radar System. The experimental results showed for the SPR and SPI processes that the affect of range side lobes will need to be studied further. Future studies will attempt to experimentally test the affect of moving targets on the SPR technique. The Experimental Array Radar System has recently been upgraded so that data collection of moving targets is now possible. While it is possible to reduce radar dwell times by implementing the SPR or SPI process, the algorithms could also be used to enhance existing HRR systems by at least doubling the target size they could identify.

Riseborough, E. S., and Wilkinson, A., New Stepped Frequency Waveform Algorithms for High Range Resolution Radar: Short Pulse Reconstruction and Short Pulse Identification, Defence Research Establishment Ottawa, DREO TR2000-011, February, 2000.

Sommaire

Un des problèmes rencontré par les concepteurs de radar multifonctions (RMF) est un budget limité en temps. Un RMF doit effectué plusieurs fonctions en parallèles, tel que la surveillance d'horizon, l'engagement de cibles, la cartographie du fouillis, et des fonctions qui prennent beaucoup plus de temps tel que la haute résolution en portée (HRP) d'un radar. La HRP est considérée comme un ajout potentiel pour les RMF présentement en développement. Les concepteurs doivent donc définir la forme d'onde requise pour la HRP dès le début de la conception du RMF et inclure cette capacité quand le RMF est construit. Ceci simplifiera l'installation de la fonction HRP quand le RMF sera prêt. Pour cela, on doit choisir la grandeur maximum de la cible que le système HRP pourrait identifier, et la forme d'onde requise pour cette tâche. Deux formes d'ondes peuvent être utilisées pour accomplir la HRP, la compression de pulse et la modulation discrète en fréquence. La compression de pulse à la capacité d'obtenir la signature HRP en une seule pulse. Ceci exige la transmission d'une longe pulse, d'une durée de centaines de micro secondes, et un récepteur avec un filtre adapté pour extraire le profile en portée. Un RMF doit effectuer plusieurs fonctions lesquelles ne demande pas de si longue pulse. De plus, la compression de pulse avec de très large bande (de l'ordre de centaines de MHz) augmente la complexité du système RMF. L'utilisation d'une forme d'onde qui ne demande pas de modification du système est préférable. Les RMF en développement sont supposées utilisées une modulation discrète en fréquence pour obtenir la HRP puisque cela est une forme d'onde relativement facile a produire due à sa bande étroite de fréquence. Fondamentalement, la forme d'onde consiste en un train de pulses qui change de fréquence pas par pas à travers une plage de fréquences. Les pulses sont intégrées à travers une transformation inverse de Fourier pour obtenir le profile haute résolution en portée (ou l'image HRP) de la cible. Un besoin essentiel de la modulation discrète en fréquence est que la pulses transmissent soit suffisamment longues pour englober la cible interrogée. Ceci pose un problème pour les grandes cibles puisque le radar aurait à transmettre des pulses encore plus longue. L'incrément de fréquence dans la modulation discrète serait alors réduit produisant un temps plus long d'illumination pour le radar. Le choix de la longueur maximum de la cible qui peut être identifier par le RMF en utilisant une forme d'onde discrète implique un processus de décision compliqué.

Ce rapport décrit deux techniques relativement simples, appelées les techniques de reconstruction et d'identification à impulsions courtes lesquelles peuvent être utiliser pour minimiser le temps requis du RMF pour effectuer la HRP. Ces nouvelles techniques utilisent des impulsions de durée plus courte pour échantillonner la cible. Ils utilisent aussi un système d'acquisition de données analogique - numérique haute vitesse qui sera déjà installée dans les RMF. La technique de reconstruction à impulsions courtes (RIC) crée l'image complète de la cible à partir des images adjacentes HRP. La technique RIC nécessite une routine pour trier les crêtes de diffusion des images adjacentes. En utilisant des impulsions plus courtes, la modulation discrète en fréquence n'a pas besoin d'un incrément de fréquence plus petit réduisant ainsi le temps d'illumination. Un autre avantage potentiel de cette technique est que puisque le temps d'illumination est réduit de moitié, ceci devrait aussi réduire la déformation due à la compensation de mouvement. Une approche alternative à la technique RIC est aussi

présentée, laquelle essaie d'effectuer l'identification de la cible sans la reconstruire. Cette approche est appelée l'identification à impulsions courtes (IIC).

Ce rapport décrit les techniques RIC et IIC, aussi bien que l'analyse des performances impliquant les compensations de mouvement et les effets sur le SNR. Les performances d'identification sont étudiées en utilisant un processus similaire à la somme des modules normalisés résiduels. La validation expérimentale de la technique RIC est présentée en utilisant différentes configurations de réflecteurs en coin.

Les simulations de ces études utilisent une banque de donnée de 100 images HRP similaires générés au hasard pour 11 angles d'orientation différents. Une comparaison est faite entre les techniques de RIC, IIC, et les techniques conventionnelles à basse et haute résolution en portée. Seules les erreurs de compensation de mouvement spécifiques (c'est à dire seulement la compensation de vitesse) ont été essayées pour chaque test en vue d'isoler les effets étudiés. L'analyse des simulations des techniques RIC et IIC ont données des résultats prometteurs. L'estimation imprécise des compensations de mouvement requise pour les HRP produit des images très déformées. Les systèmes d'identifications utilisent seulement des signatures HRP imparfaites, causant ainsi une dégradation des performances. Des formes d'onde tolérantes à la vitesse et l'accélération peuvent être utilisées pour solutionner quelque uns des problèmes de compensation. Si la compensation est parfaite alors les routines RIC et IIC fonctionnent aussi bien que les techniques conventionnelles HRP. Ces techniques sont plus sensibles au SNR, mais cela est prévu due au fait que seulement la moitié des points sont intégrés comparativement au processus conventionnel HRP. La version basse résolution de la HRP opère mieux que les autres systèmes d'identifications. Ce résultat montre l'importance de définir une bonne résolution pour l'identification HRP. Chaque cible dans la banque des signatures contient jusqu'à 16 crêtes de diffusions dispersées approximativement sur 50 mètres, et la résolution de 0.3m que la bande de fréquence de 500MHz donne peut ne pas être requise pour effectuer l'identification avec succès. Tandis que la version basse résolution travaille mieux pour ces simulations, la routine RIC a démontrée quelle pouvait reconstruire une cible a partir d'image multiples, et aussi donnée de bons résultats d'identification. Le choix d'un bon seuil d'amplitude est essentiel au succès des routines RIC et IIC. En ayant un seuil d'amplitude trop bas, le bruit ou l'erreur sur la compensation de mouvement induit des crêtes de diffusions déformant l'image finale, et réduit l'efficacité de la technique IIC pour l'identification de cibles.

La routine de triage RIC est capable de déterminer la géométrie et l'amplitude des signaux pour différentes configurations expérimentales utilisant le radar à réseau expérimental. Les résultats expérimentaux montrent que les effets des techniques RIC et IIC sur lobes auxiliaires en portée ont besoin d'être étudier davantage. Des études futures vont essayer de tester expérimentalement les effets de cible mobiles sur la technique RIC. Récemment, le système radar expérimental à réseau a été amélioré pour pouvoir collecter des données sur des cibles mobiles. Les techniques RIC et IIC peuvent être utiliser pour réduire le temps d'illumination, aussi bien que pour améliorer les systèmes existant de HRP en doublant la grandeur des cibles qui peuvent être identifier.

Riseborough, E., Wilkinson, A., <u>Nouveaux algorithmes de modulation à fréquences discrètes pour des radars à haute résolution en portée : La reconstruction par impulsions courtes et l'identification par impulsions courtes</u>, Le Centre de recherche pour la défense Ottawa, DREO TR2000-011 , Février, 2000 (en anglais).

TABLE OF CONTENTS

LIST OF FIGURES

1.0 Introduction

One of the problems facing Multi-Function Radar (MFR) designers is a limited time budget. An MFR has to perform many functions in parallel, such as horizon search, target engagement, clutter mapping and time-consuming functions, such as high range resolution radar (HRR). As HRR would be considered as a growth items for MFR's presently under development, the designers have to define the waveforms required by the HRR and include this capability in the MFR when it is built. This simplifies the installation of the HRR feature when it is ready. To do this involves selecting the maximum target size that the HRR system could identify, and the waveform to perform this task. Two waveforms can be used to achieve high range resolution, the pulse compression and stepped frequency waveforms. Pulse compression has the ability to acquire the HRR signature in one pulse. This requires a long transmitted pulse, of duration of hundreds of microseconds, and a matched filter receiver to extract the range profile. An MFR has many other functions to perform which don't require such a long pulse, to add pulse compression with very wide bandwidth (in the order of hundreds of Megahertz) adds complexity to the design, and using a waveform which doesn't require modification to the hardware is preferred. MFR's under development are planning to use the stepped frequency waveform [1] to implement HRR since it is a relatively simple waveform to implement because of its use of narrow bandwidth pulses. Basically, the waveform consists of a train of pulses that step across a wide frequency band. The pulses are then integrated via an inverse FFT to get a high range resolution amplitude profile, or HRR image, of the target. An essential requirement of this method is that the radar pulse be wide enough to encompass the target being interrogated. This poses a problem in larger targets since the radar would have to transmit a longer pulse, then the frequency step size in the stepped frequency waveform would have to be reduced. This results in a long dwell time for the radar. Defining the maximum target size that can be identified before the HRR is actually in the MFR involves a complicated decision process.

This report describes two relatively simple techniques, called the short pulse reconstruction technique and the short pulse identification technique, which can be used to get the most out of the limited time budget that an MFR could schedule for performing HRR. The new techniques presented here use a smaller pulse width to sample portions of the target, and make use of high-speed analog-to-digital data acquisition systems that should already be part of the MFR. The Short Pulse Reconstruction (SPR) technique would create the complete target image based on adjacent overlapping HRR images. The SPR technique requires a routine for sorting the peak scatterers from the adjacent images. By using reduced pulse widths, the stepped frequency waveform would not require the smaller frequency step size; therefore, the radar dwell time is also reduced. Another possible advantage of the technique is that since the radar dwell time is reduced by at least half, this should reduce the motion compensation related distortions as well. An alternative approach to the SPR technique is also presented, which would attempt to perform identification on a target without reconstructing the target. The approach is called short pulse identification (SPI).

1

This report will describe the SPR and SPI techniques and present the analysis performed on the them involving motion, and signal to noise ratio effects. This involved the creation of a database of 100 randomly generated, but similar target images at 11 aspect angles. A comparison is made to the conventional HRR process for target identification using a process similar to the sum of the moduli of normalized residuals (MNR) process [2]. A low resolution version of the conventional process is also used in the study.

An experiment was performed in 1998 using several corner reflectors as targets to test the short pulse reconstruction process. Observations of the experimental data led to some refining of the SPR algorithm. The refinements consider unwanted side-lobes in the images.

2.0 Short Pulse Reconstruction Technique for Creating an HRR Image

HRR signal processing conventionally uses a stepped frequency waveform to achieve a wide bandwidth [1]. This waveform is a train of radar pulses that are stepped in frequency, ΔF, through a series of N frequencies encompassing a frequency bandwidth, B.

$$B = N \Delta F \tag{1}$$

The range resolution, ΔR, of the stepped frequency waveform is inversely proportional to the bandwidth, that is, the wider the bandwidth the higher the resolution.

$$\Delta R = K \left(\frac{c}{2B} \right) \tag{2}$$

K is a constant determined by the signal processing effects and is equal to or greater than unity and c is the speed of light. The radar pulse width, τ, must also encompass the entire target being sampled, (R_t).

$$R_r = \frac{c}{2\tau} \tag{3}$$

Once target data is collected at all frequency steps, an inverse FFT is used to create high resolution amplitude versus relative range plot. The unambiguous range of the HRR image (R_u) is inversely proportional to the frequency step size, that is, the larger the step size the smaller the unambiguous range.

$$R_u = \frac{c}{2\Delta F} \tag{4}$$

The unambiguous range of the HRR image is the maximum target length that can be generated with the stepped frequency waveform.

2

Therefore, if you wish to generate an HRR image of a 60-metre target with 1 metre resolution, you would require at least a 400 ns radar pulse width, a frequency step size of 2.5 MHz, and a bandwidth of 150 MHz. At a pulse-repetition-frequency of 1 KHz this would take 60 ms to collect the data. If time constraints were imposed, the HRR radar designer would have to investigate several options to meet the time budget. If the conventional stepped frequency waveform approach is used, then to meet the time budget the radar would have to reduce bandwidth at a cost of range resolution, or increase the frequency step size at a cost of unambiguous range window size. Reducing the range window size limits the target size that may be examined. Increasing the pulse repetition frequency, PRF, will reduce the dwell time. This will increase the cost of the frequency synthesizer in the radar, as it will have to switch frequencies faster. Also, raising the PRF also reduces the unambiguous range of the radar, not to be confused with the unambiguous range of the HRR image. To create an HRR image of targets at ranges beyond this unambiguous range requires the radar to store the phase of each frequency pulse to be used to down convert each radar return to baseband. While this is possible, it is quite complex and would require a substantial modification to the overall MFR design.

A modification of the conventional stepped frequency technique can be used to reduce the time budget of the radar without sacrificing its range resolution or its unambiguous range of the HRR image. The proposed technique, called the short pulse reconstruction technique, builds a target HRR image from overlapping partial target HRR images. To create the HRR image this technique requires a high speed analog to digital (A/D) system, a narrow radar pulse width which is less than the maximum required target size, and a sorting routine. If the radar has a pulse width pw and it scans a target of length (pw x 2) centred at range R, the high speed A/D system would have to sample the target at range (R-pw/2), R, and (R+pw/2) for each frequency step. The unambiguous range for each of the sample sets would be reduced by a factor of 2, thus increasing the frequency step size by 2, which in turn reduces the dwell time required to create the image by one half. An image is then generated for each data set. Each set will contain an amplitude versus relative range image that could be wrapped around thus creating three range ambiguous plots. Since the pulsewidth only encompasses one half of the target, the first data set would be of the first half of the target; the second data set would be from one quarter to three quarters of the target, and the third would be of the second half of the target. Figure 1 shows a conventional image of a target sampled with a 400 ns pulse width and step size 2.5 MHz. Figure 2 shows three overlapping conventional images of the same target sampled with a 200 ns pulse width and a step size of 5 MHz. The difficulty evident with both Figures is in determining where the target starts and ends as the HRR images could be wrapped around in the range window. For this example, Figure 1 is unwrapped to simplify the description of the SPR technique.

The second data set in Figure 2 would be used to sort out the first and third data sets. This is done by comparing the location of the peaks of the images of sets 1 and 3 with set 2 to determine the location of the scatterers in the second set.
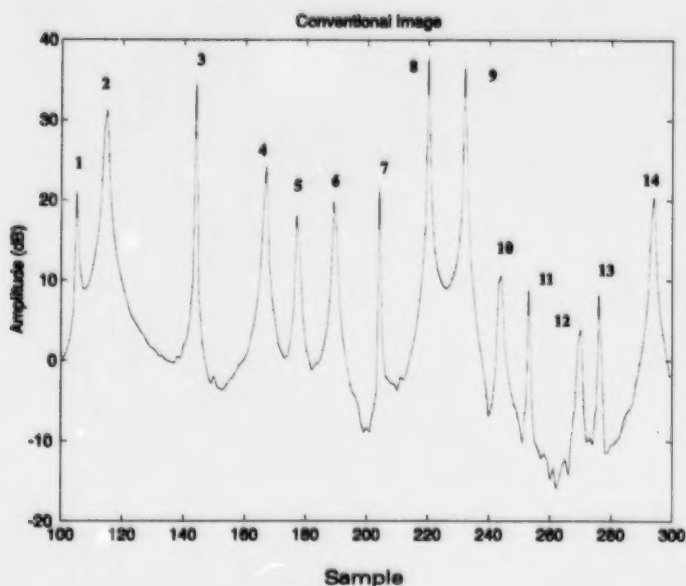
Figure 1: HRR Image of a Sample Target using the Conventional HRR Process.

The unmatched scatterers would therefore lie outside the range of set 2. For data set 1, the first scatterer rotating to the right of the last matched scatterer with set 2 would be the first major scatterer of the target. For data set 3, the first scatterer rotating to the left of the first matched scatterer with set 2 would be the last major scatterer of the target. The sorting routine would have to take into account the wrap around of the images to determine what are the last matched scatterer of set 1 and the first matched scatterer of set 1. Both images can then be rotated and put adjacent to each other, thus creating a widened image. Finally, data set 2 would be used to determine the distance between the last scatterer of the first half of the image and the first scatterer of the second image. Also, adding noise to the HRR inputs would add spurious peaks to the HRR image, therefore, a threshold must be added to the sorting algorithm to reduce the noise effects. To further explain the algorithm, in Figure 2, image 1 has 3 peaks that match in relative range with image 2. These are labelled 4, 5, and 6 in the Figure. Therefore, we assume that the remaining peaks in image 1 lie in the first half of its image. Image 3 has 4 peaks that match in relative range with image 2. These are labelled 7, 8, 9, and 10. Therefore, we assume that the remaining peaks in image 3 lie in the second half of its image. Finally, the distance between peak 6 and 7 is evident in image 2. The resulting reconstruction is shown in Figure 3, which matches up well with Figure 1. Since each of the partial target images was created using one half of the frequencies of the conventional approach, the signal to noise ratio of the HRR image would be reduced by 3 dB from that of Figure 1. While the peak values are not affected in the figures, the noise floor of Figure 3 is higher than that of Figure 1. Note that this is a simplified case where only image 2 of Figure 2 actually displays the wraparound effect. The sorting routine must perform this reconstruction automatically, and operate in the case that all three images are wrapped around as well.
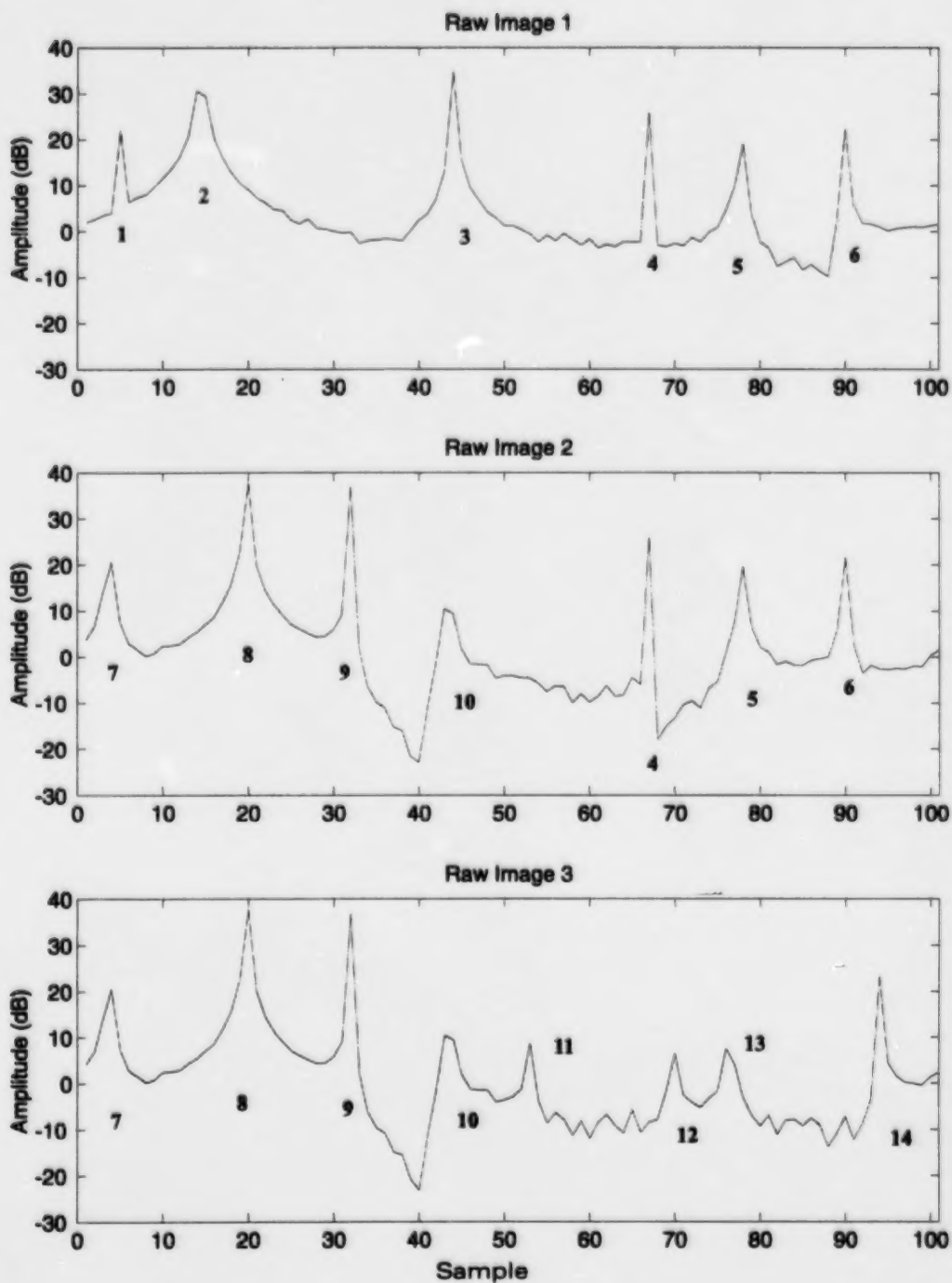
4

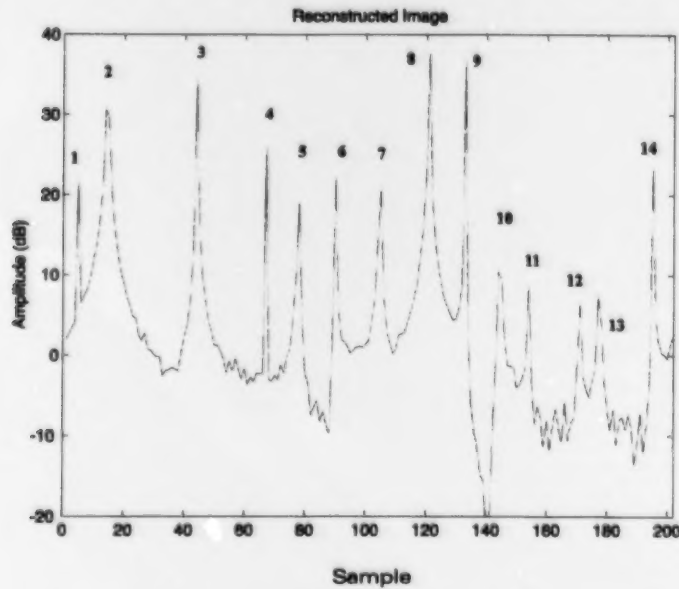Figure 2: Overlapping Images of the Sample Target.

Figure 3: Reconstructed Image of Sample Target

The reason that the approach would work lies in the answer to the question, "Why should the peaks be in the same location in the overlapping images?" The reason is in the requirement that the data must be collected by a system that can collect all the required range bins in each pulse. In the reconstruction case just demonstrated, the time between the samples for each frequency, Δt, was 100 ns. This corresponds to a sampling rate of 10 MHz. It should be noted that 12-bit A/D systems are capable of sampling rates above 20 MHz, which the system used to collect the experimental data for this report is capable of. Therefore, the three images would be created using the same radar pulse at each frequency. Taking the example of a point source being sampled for image 1 and image 2. While there is a time delay of Δt between the individual frequency samples for image 1 and image 2, the signal is mixed to baseband against a stable local oscillator offset by the same time delay. This results in the same return for each target at each frequency. After an inverse FFT is performed, and an amplitude of the data is taken, the resulting peak would be at the same location for the two images. On March 6, 1997, experimental data was collected on the Ottawa River when it was frozen over to verify the SPR concept. Figure 4 shows one radar pulse taken of a corner reflector on the ice at 8.9 GHz. The radar was stepped in frequency from 8.9 to 9.4 GHz in step sizes of 5 MHz. An HRR image was created using the peak in the figure, as well as the two adjacent points. Figure 5 shows that the HRR images line up in relative range. Figure 6 shows the potential problem of using the overlapping technique, as a spurious peak is present. It is approximately 20 dB down from the main peak.
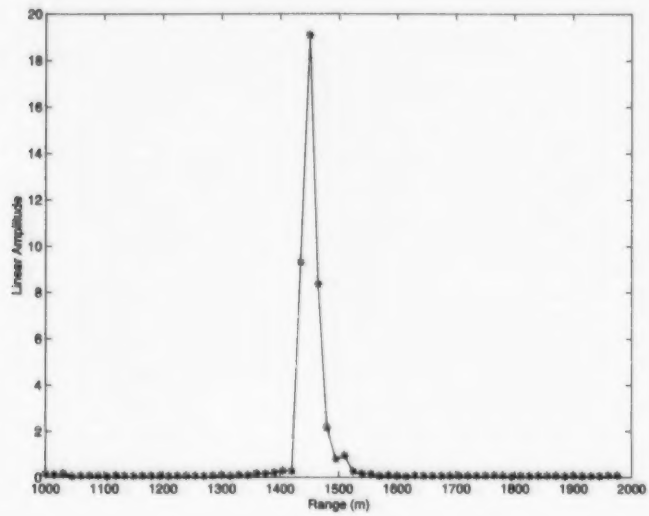
6

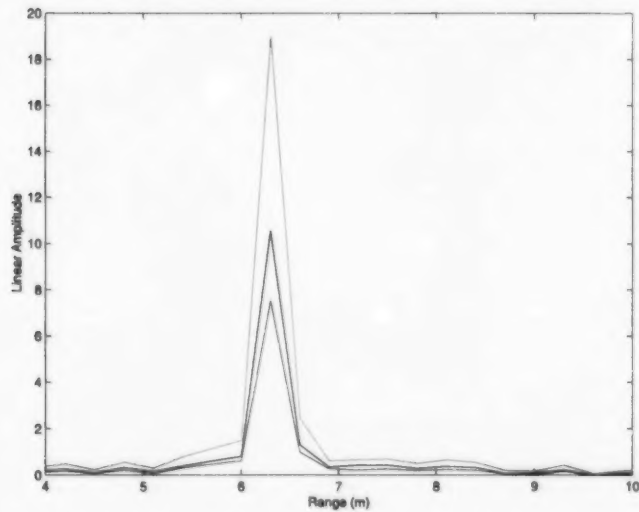**Figure 4: Standard Return (no HRR processing) of Corner Reflector Situated on Ice.**

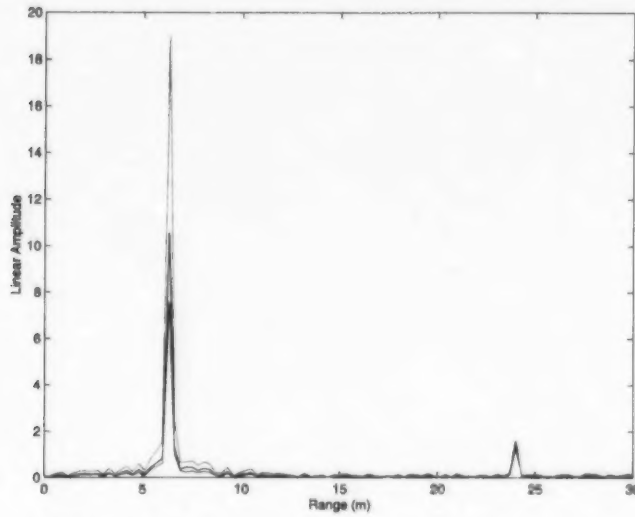**Figure 5: High Range Resolution Return from Three Overlapping Range Cells of Corner Reflector Situated on the Ice.**

7

Figure 6: Expanded Image of SPR Technique, Sidelobe may Introduce Problems.

3.0 Target Identification

A simple way to perform target identification is to compare a Library image, L, with the target image, T, by performing a series of operations. First, for each point in image L, subtract the corresponding T value and then sum the absolute values of the differences. Next, rotate L one position and perform the sum of the differences again. Repeat this process until L has been completely rotated. The minimum of these sums would be used as an identifier. Finally, this process would be performed for a whole library of images, storing each value in vector C. The minimum value of C would then be selected as the potential target. This process is similar to the sum of the moduli of normalized residuals (MNR) process described in [2]. Both target and library images should be normalized with respect to the largest return in each image. In the HRR image there is can be a wraparound of the target. Since the target image can be wrapped around, the rotation involving the library file must wrap around as well. Equation 5 displays the process.

$$C(m) = \sum_{n=0}^{N-1} \left| \frac{L(modulo_N(n+m-1)+1)}{MAX(L)} - \frac{T(n+1)}{MAX(T)} \right| \tag{5}$$

where: m= 1 to N

$modulo_N(I) = I - N \times [\ INTEGER(I\ /\ N)\ ]$

While the above equation works, it is complicated and can't easily be implemented for

8

vector comparisons that high speed processors could make use of. A modification would be to store the library vector twice into a larger vector, LB, thus removing the requirement of worrying about the wrap around effect of the images on the equations. Using a normalized LB and T, Equation 5 becomes:

$$C(m) = \sum_{n=0}^{N-1} \left| LB_{norm}(n+m) - T_{norm}(n+1) \right| \qquad (6)$$

where:
$$LB(I) = L(I), \text{ for } I = 1 \text{ to } N$$
$$LB(N+I) = L(I), \text{ for } I = 1 \text{ to } N$$
$$LB_{norm} = LB / MAX(L)$$
$$T_{norm} = T / MAX(T)$$

The minimum value of C would correspond to the best match for a particular target, and would be saved for further comparison as $C_{min}(i)$. This process would be repeated on each target stored in a library data set. The minimum of the C_{min} values would identify the most likely target from the library data set. At this point the identification process is completed. Setting values that are less than the threshold to zero is considered as an option, since the side lobe due to the dominant peak in the large image will increase the noise floor. The noise floor in the small image that does not include the dominant peak will be lower due to the side lobe level being lowered as well.

Other processes that could be used to perform the template matching use cross correlation[3]. These were not studied here, as the main purpose of this report is to study the effect of the short pulse techniques on identification.

4.0 Short Pulse Identification

For complex targets, such as aircraft, aspect angle has a detrimental effect on the reconstruction process. If one tests reconstruction of a target by rotating it from 0 to 90 degrees, the sorting routine will have problems at the edges of the middle image at several aspect angles. At these aspect angles two of the major scatterers in the target would be separated by the ambiguous range of the HRR process, resulting in one peak in the middle image, when there should be two. This will cause the sorting routine to break down. It will not be able to determine which is the start or end peak as they are overlapped. By setting the threshold properly this problem can be avoided. However, if the overlapping scatterers are of sufficient strength, for example, the strongest, then the reconstruction will fail. As this will occur at only a few aspect angles for any given target and the probability that the largest peaks overlap is low, then this problem should have a very low probability of occurring. If the sorting routine flags the problem a secondary HRR data collection could take place. The Short Pulse Identification (SPI) process alleviates this problem. An alternative to the SPR technique is to bypass reconstructing the target image entirely and move directly to the identification process. Once again a short radar pulse is

9

used, however, only the first and third images from the SPR scenario are used for identification. This will save time in sorting the returns, and reduces the edge effect problems of the radar pulse.

The identification is performed using a library of M targets. The library set will consist of standard images L(M). There are two sources one can utilize for creating a library of images. One method is to collect data experimentally; the other is to generate the data via modelling. Collection of HRR images experimentally has two major drawbacks. One is the difficulty in getting experimental data from targets not in our arsenal, and the other is the time consuming data collection process that would be involved in collecting a particular target image. Target aspect angle with respect to the radar will have to be precisely known, and the target will have to measured at possibly hundreds of aspect angles to ensure an adequate library of images are available to perform an identification. Motion compensation will also have to be performed to generate each image as well. Generating library images via target modelling would be the preferred approach; however, some experimental data would still have to be collected for model validation.

In the absence of a library of "true" targets, simulated targets of point scatterers will be used here. The procedure for generating the library is outlined below. It should be noted that this procedure is useful for generating a library test set, as it can be done automatically. In reality, targets that are modelled or collected would have to be "unwrapped" by examining the data sets as precise geometry and amplitude gains would not be available.

In creating the library of images for use by the identification technique, one must make sure each image is "unwrapped." One method is to use the known geometry and reflector powers to determine if the image is unwrapped. First, you would generate an amplitude plot of the HRR library image. Next, you would find the number of peaks in the image. The image would have peaks shown in relative range rotating from left to right. Any peak in the image could correspond to the true start of the target. Therefore, the first peak found by rotating to the left of this target could correspond to the true end of the target. The range between the all the peak pairs is then found by rotating to the right.

The peak pair that best matches the range between the end peaks from the known geometry of the target is determined by an iterative search of all the peak pairs. If there were more than one set of peak pairs that closely match the true range difference (since we would be working with a large database with many aspect angles for each target), a secondary comparison would be required. The secondary comparison uses the ratio of the amplitudes from each peak pair to compare with that of the true amplitude ratio from the database. The comparison must take into account the resolution of the HRR radar and add in the reflector powers of those that lie within the resolution bounds. The closest match would give a value nearest to 1, which would give the target's most likely starting and finishing peak. From this the centre of the image is found. Finally, the image is then rotated to the right until the centre of the image is centred for the database.

Once the library file is available target identification can take place. The short pulse identification process is described below.

First, two images (R1 and R2) which are the result of the stepped frequency waveform of a narrow pulse width sampled at a separation of one pulse with (i.e. Images 1 and 3 from short pulse reconstruction process) are created. The two images are normalized to the maximum peak of the two images. A threshold is selected as an input for the identification process.

For each target in the library, L(I), the following process will take place:

(1)   The number of peaks in R1, N1, that are above the threshold is found. The first N1 peaks of image L(I) above the threshold is used. Fill the remaining data after the last peak with zeros. This sets the subset of L(I) to have the same length as R1. The MNR process is then performed, with result C1.

(2)   The number of peaks in R2, N2, that are above the threshold is found. The last N1 peaks of image L(I) above the threshold is used. Fill the remaining data after the last peak with zeros. This sets the subset of L(I) to have the same length as R2. The MNR Process is then performed, with result C2.

(3)   The sum of C1 and C2 is saved in SUM(I).

After all the library files have been examined the minimum value of SUM should correspond to the target. Some rules that are required by the Identification Algorithm follow:

(1)   If either smaller image has more peaks than the bigger image, then reject the larger image as a possible target.

(2)   If the larger images first N peaks has a spread greater than that of the small image 1 size then reject the larger image as a possible target. The same rule applies to the small image 2 with last N peaks of the larger image.

(3)   The library images are assumed to be unwrapped.

11

5.0 Low Resolution HRR Approach

The simplest method of saving radar dwell time is to reduce the bandwidth of the stepped frequency waveform. For comparison purposes, the dwell time will be the same as that of the SPR and SPI routines. The process is: use the same waveform as for the conventional HRR process, however, use only half the bandwidth, and use zeros to fill up to the same number of points as required by the conventional HRR process. Everything else is the same including the MNR process. By only using half the bandwidth, the range resolution is halved and the SNR is reduced by 3 dB. This approach was initially included in the study to show the effect of lowering the range resolution on target identification. The results in the next section will show that defining the resolution requirements is not an easy task, as the "low resolution" was sufficient for handling all the scenarios. Further investigation into resolution requirements for successful target recognition should be made before arbitrarily setting a value. The results are included here for archival purposes.

6.0 Target Simulations

The simplest form of representing a target scatterer considers a point source at range R_S, which has a return power of P_S. For a transmitter of frequency f_n, the return signal, Y_S, of the target would be

$$Y_S = P_S e^{-j\varphi_n} \tag{7}$$

Next, consider a complex target with many major scatterers. Equation 7 would be repeated for each scatterer in the target, resulting in one complex return for each frequency, $n=1,2,....,N$, in the stepped frequency waveform. Where m represents the returns from the major scatterers, and M is the number of major scatterers.

$$Y(f_n) = \sum_{m=1}^{M} P_{S(m)} \ e^{\frac{-j4\pi R_{S(m)} f_n}{c}} \tag{8}$$

Equation 8 represents the return from a complex stationary target. For each scatterer in a complex moving object, $R_t(n)$ would change as a function of time. Consider an aircraft flying at velocity of V_0 with a trajectory of θ_0 with respect to the HRR radars pointing direction. A simple representation of an aircraft is an inverted T formation with scatterers located along its formation as displayed in Figure 7.
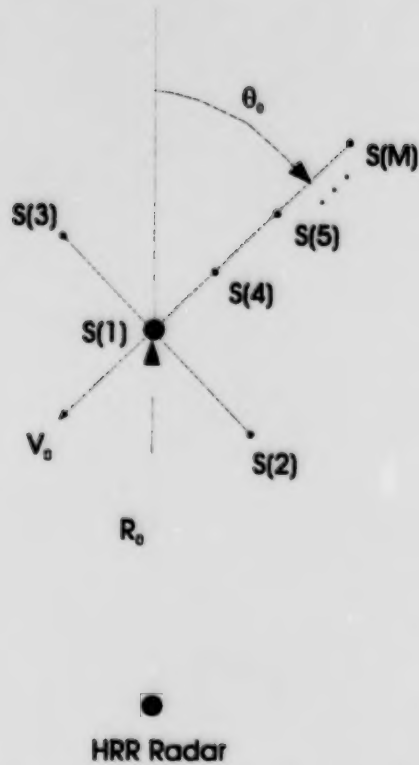
Figure 7: Simulated Target Geometry

S(1) would represent the scatterer at the centre of the "wings". Using this scenario the range, $R_{S(1)}$, with respect to time for S(1) is

$$R_{S(1)}(t) = \sqrt{((V_0 t + A_0 t^2/2) \sin\theta_0)^2 + (R_0 - (V_0 t + A_0 t^2/2) \cos\theta_0)^2} \tag{9}$$

where: R_0 = Initial Range in metres from S(1) to HRR Radar as shown in Figure 4.

t = time of sample in seconds
  = t_0 + (n-1)/PRF
t_0 = initial time of sample 1.
A_0 = acceleration on target in m/s^2
PRF = pulse repetition frequency in Hz

13

The range of the scatterers along the aircraft is given by

$$R_{S(m)}(t) = \sqrt{((d(m) - V_0 t - A_0 t^2/2) \sin\theta_0)^2 + (R_0 + (d(m) - V_0 t - A_0 t^2/2) \cos\theta_0)^2} \qquad (10)$$

where $d(m)$ = distance of scatterer $S(m)$ from $S(1)$. The range of the wing tip scatterers, $S(2)$ and $S(3)$, are given by

$$R_{S(2)}(t) = \sqrt{(d(2) \cos\theta_0 - (V_0 t + A_0 t^2/2) \sin\theta_0)^2 + (R_0 - d(2) \sin\theta_0 - (V_0 t + A_0 t^2/2) \cos\theta_0)^2} \qquad (11)$$

$$R_{S(3)}(t) = \sqrt{(-d(3) \cos\theta_0 - (V_0 t + A_0 t^2/2) \sin\theta_0)^2 + (R_0 + d(3) \sin\theta_0 - (V_0 t + A_0 t^2/2) \cos\theta_0)^2} \qquad (12)$$

Now, each of these scatterers has its own radar cross section (RCS). These range values, and associated RCS would then be substituted into Equation 6. While in simulations it is simple to perform motion compensation on each scatterer, this can not be performed in reality. The best motion compensation to be expected would be to apply a similar phase shift to all parts of the target based on estimated starting target range, R_{comp}, velocity, V_{comp}, and heading, θ_{comp}, to determine a compensated return, Y_{comp}. These would be obtained from tracking algorithms from other systems or subsystems of the HRR radar itself.

$$Y_{comp}(f_n) = Y(f_n) e^{\frac{-j4\pi f_n}{c}\left(R_{comp} - \sqrt{(V_{comp} t \sin\theta_{comp})^2 + (R_{comp} - V_{comp} t \cos\theta_{comp})^2} \right)} \qquad (13)$$

$V_{comp} t \cos\theta_{comp}$ has a first order effect on the phase, $V_{comp} t \sin\theta_{comp}$ has a second order effect on the phase. As target identification is performed on targets at far ranges, $V_{comp} t \sin\theta_{comp}$ will tend to 0. This simplifies equation 13 to

$$Y_{comp}(f_n) = Y(f_n) e^{\frac{-j4\pi f_n}{c}\left(V_{comp} t \cos\theta_{comp} \right)} \qquad (14)$$

By having the target move at velocity V_0 and heading θ_0 with imperfect compensation or with no compensation for acceleration, the short pulse techniques will be compared with the conventional technique to see which technique would degrade more quickly.

14

6.1 Simulation Scenarios

The pulse repetition frequency of the simulated radar will be 2 KHz. This is selected to extend the unambiguous range of the radar to 70 kilometers, and to simplify the processing required to determine target range. The bandwidth for SPR, SPI, and conventional HRR will be from 8.9 to 9.4 GHz. These frequencies match those of our experimental radar. For low resolution HRR, the bandwidth will be 8.9 to 9.15 GHz. The frequency step size for the conventional and low resolution HRR will be 2.5 MHz with a pulsewidth of 400 ns. The frequency step size for SPR and SPI will be 5 MHz with a pulsewidth of 200 ns.

A library of 100 targets is used for the testing of the algorithms. The length of each target is 50 m having 6 to 14 scatterers with return power from -10 to 20 dB. The wing scatterer for each target is at 20 meters from the body with a power of 15 dB. The simulated targets will have a velocity of 300 m/s at a trajectory of 30 degrees starting at a range of 35 km. The trajectory of 30 degrees was selected, so as to rotate some of the targets sufficiently to cause edge effect problems with the short pulse methods. Motion compensation effects will be tested by compensating incorrectly for velocity and trajectory. A second set of tests will add acceleration to the simulation without performing compensation for acceleration. Finally, the signal to noise ratio will be tested with perfect compensation. The library will have 11 rotations of the 100 targets with aspect angles from 29 to 31 degrees in .2 degree increments.

6.2 Perfect Compensation Tests

Four targets were selected randomly from the database to test the algorithms, targets 5, 23, 66 and 77.

Target 5 Scatterer Type	Scatterer Position from Front (M)	Scatterer Power (dB)
Wing	-9.9957	15.000
Body	0.000	-8.057
Body	9.0529	2.705
Wing	10.0043	15.000
Body	16.4480	5.465
Body	19.9681	-3.222
Body	22.9444	19.650
Body	24.5902	7.394
Body	27.7390	7.484
Body	29.4854	2.987
Body	33.9242	0.019
Body	43.3102	12.811
Target 23 Scatterer Type	Scatterer Position from Front (M)	Scatterer Power (dB)
Wing	-9.9957	15.000
Body	0.0000	-7.368
Body	9.6090	-0.924
Body	9.8749	-9.573
Wing	10.0043	15.000
Body	22.6083	12.784
Body	30.4747	15.555
Body	30.8939	6.738
Body	35.3484	3.304
Body	40.4035	18.492
Body	42.3182	0.989
Body	43.3102	7.885
Target 66 Scatterer Type	Scatterer Position from Front (M)	Scatterer Power (dB)
Wing	-9.9957	15.000
Body	0.0000	14.294
Wing	10.0043	15.000
Body	10.4673	18.035
Body	14.3891	10.605
Body	20.3007	9.417
Body	20.6463	-1.083
Body	28.5897	-6.136
Body	30.5718	3.913
Body	43.3102	17.684
Target 77 Scatterer Type	Scatterer Position from Front (M)	Scatterer Power (dB)
Wing	-9.9957	15.000
Body	0.0000	13.664
Body	4.9581	6.128
Wing	10.0042	15.000
Body	13.8209	17.576
Body	18.9564	9.033
Body	25.6288	9.793
Body	26.9308	13.415
Body	38.7427	-0.199
Body	43.3102	12.162

Table 1: Simulated Target Geometries, Targets 5, 23, 66, and 77 of Library file

16

Figures 8 to 19 show the "perfect compensation" study for each of the targets. Each of the targets is examined in 3 figures each. Figures 8 (target 5), 11 (target 23), 14 (target 66), and 17 (target 77) display the overlapping images used by the SPR and SPI techniques. There are three overlapping amplitude versus range images displayed in parts a, b and c of each of the figures. By examining these images, the possible problems can be predicted, thresholds can be set. Once a proper threshold was selected that worked for each technique, the same threshold was used for the rest of the tests. Examination of Figure 11 (target 23) shows a potential problem for the SPR routine, where around the 20 meter range a scatterer occurs in each of the three images. Figures 9, 12, 15, and 18 displays the Library image (a), the conventional image (b), the reconstructed image (c), and the low resolution image (d) for each of the targets. The Library images and the reconstructed images are both 'unwrapped', where the scatterers are shown in order. Table 1 was used to verify that the images were unwrapped. The conventional and low resolution images are unwrapped. By examining Figure 12 a, one can see that the small scatterer near 20 meters of Figure 11 (a) is not related to the associated scatterers in b and c. As this may cause problems with the SPR routine, the threshold is set to be at 0 dB for all the SPR studies. Each of the targets will have similar problems with edge effects.

Target identification results using MNR are shown in Figures 10, 13, 16, and 19 for the conventional HRR (a), low resolution HRR (b), SPI (c), and SPR (d). Table 2 displays the identification results. The target selected and the trajectory angle is shown in most of the columns. A visual inspection of the SPR images was used to determine if the reconstruction process was successful. All the targets were identified properly by each algorithm, however, the aspect angle identified was not the same as the input trajectory. This is due to the compensation being associated with the complete target, not the individual scatterers.

	Conventional	SPR results	SPR Redraw	SPI Results	Low Resolution
Target 5	5/30.4	5/29.2	yes	5/30.4	5/30.6
Target 23	23/30.4	23/29.4	yes	23/30.2	23/30.6
Target 66	66/30.8	66/30.2	yes	66/30.2	66/30.4
Target 77	77/30.4	77/30.2	yes	77/30.2	77/30.6

Table 2: Identifier Results for Perfect Compensation

The SPI plots in Figures 10, 13, 16, and 19, have a "choppy" characteristic. This is due to the rules for implementing the short pulse identification procedure, which causes the library target to be rejected before the MNR process takes place for many cases. The MNR value assigned for a rejected target is high, to prevent rejected targets from being selected.
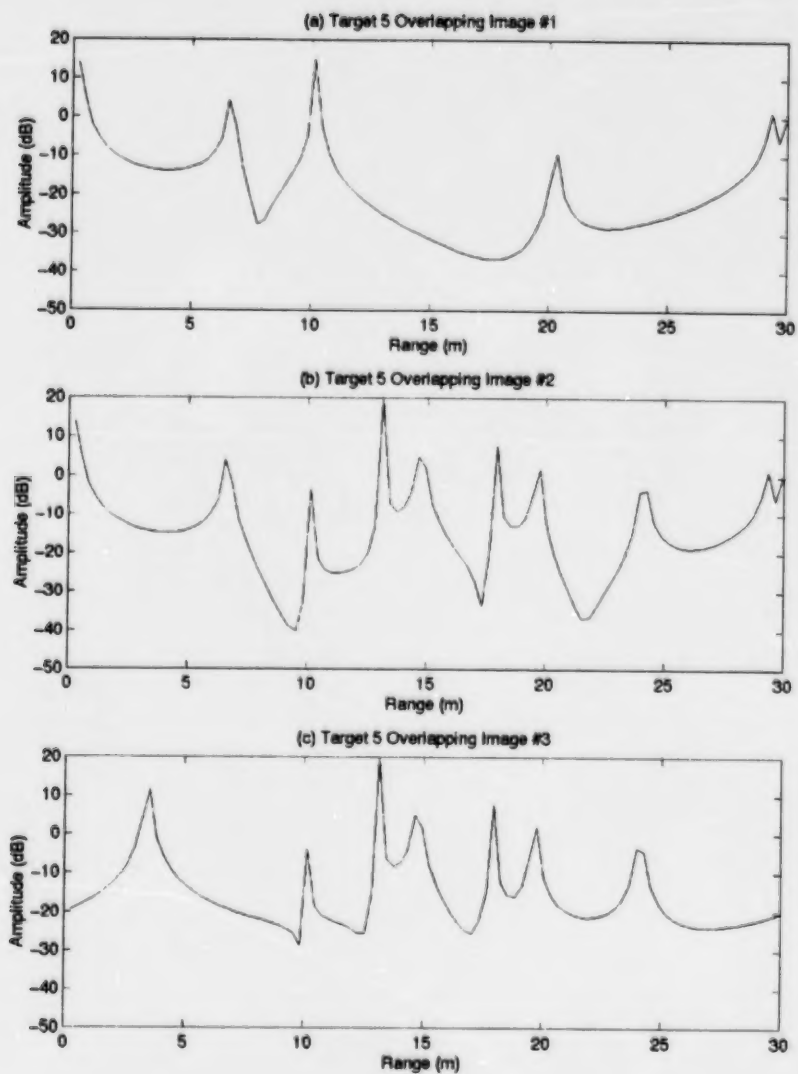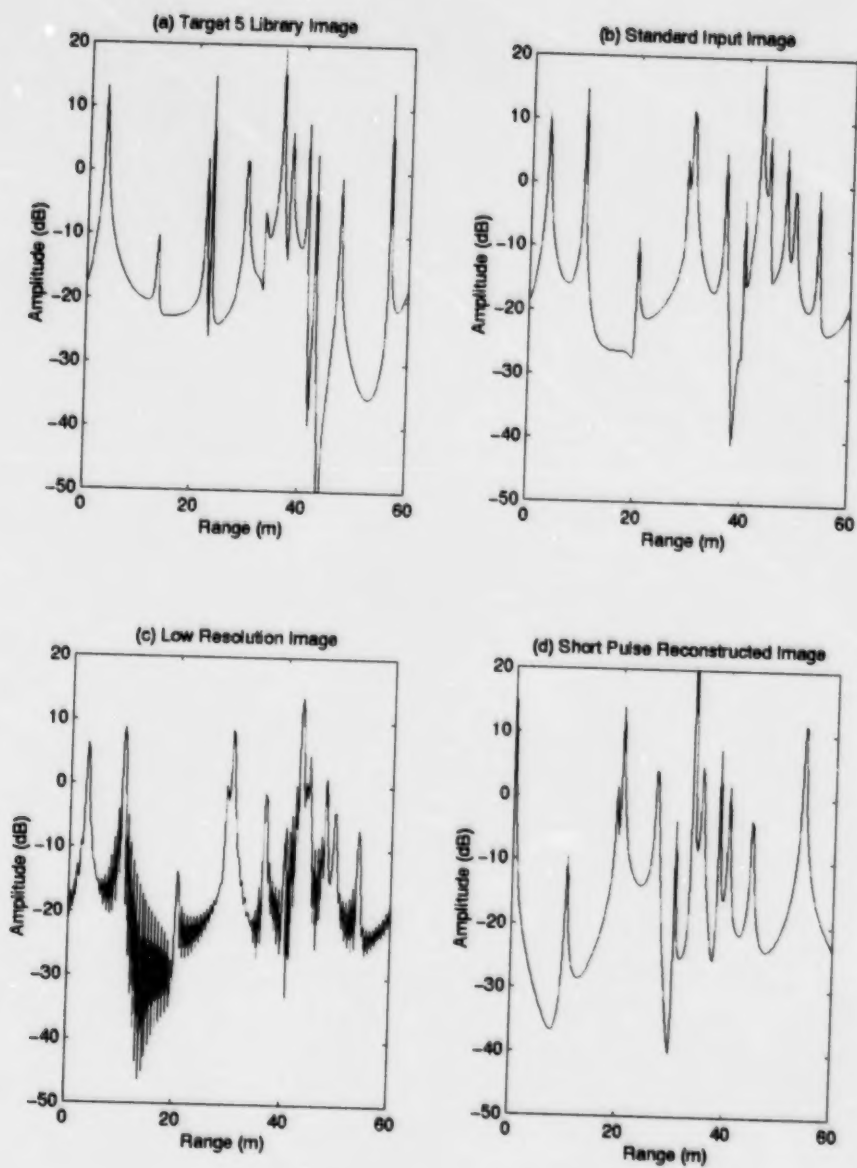
Figure 8: Overlapping Images for Target 5
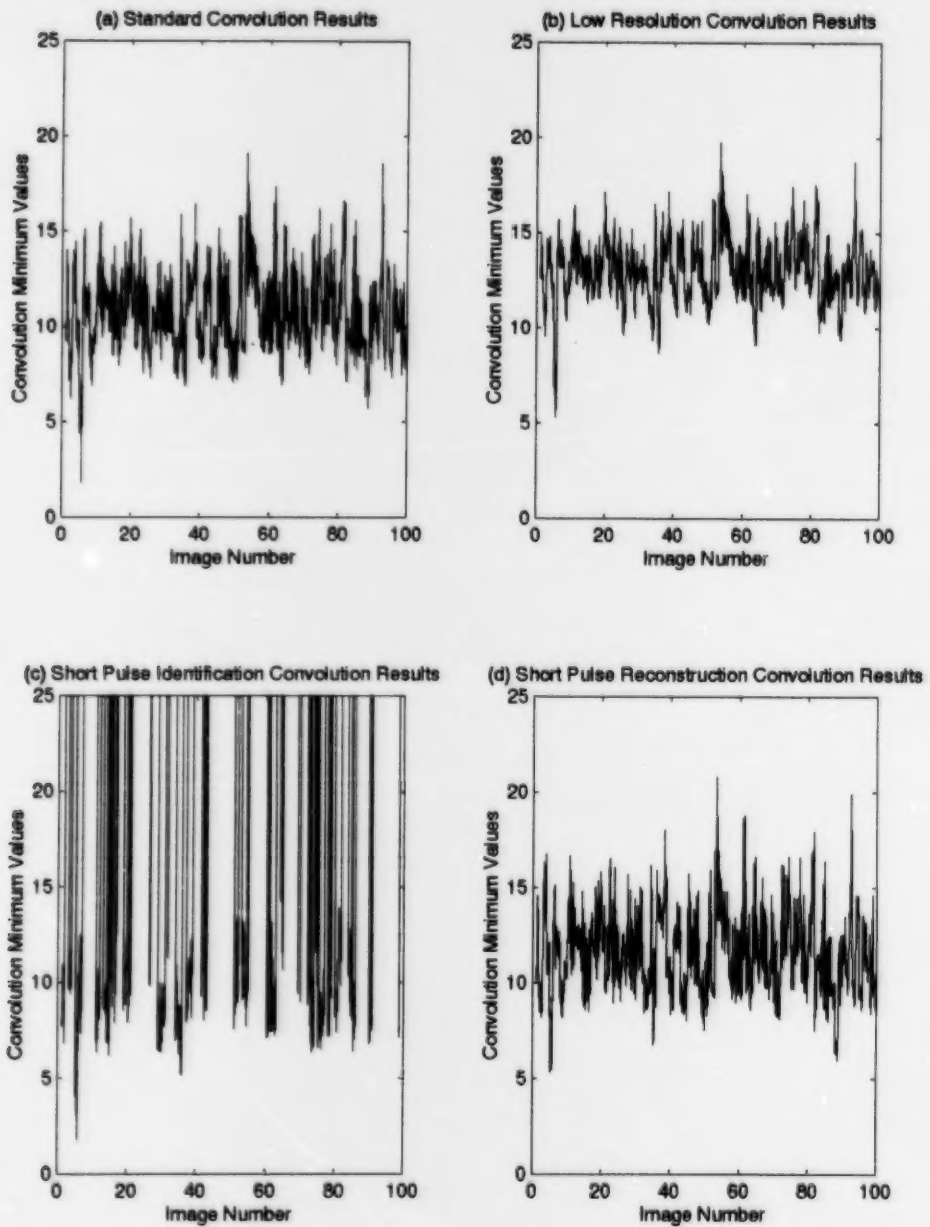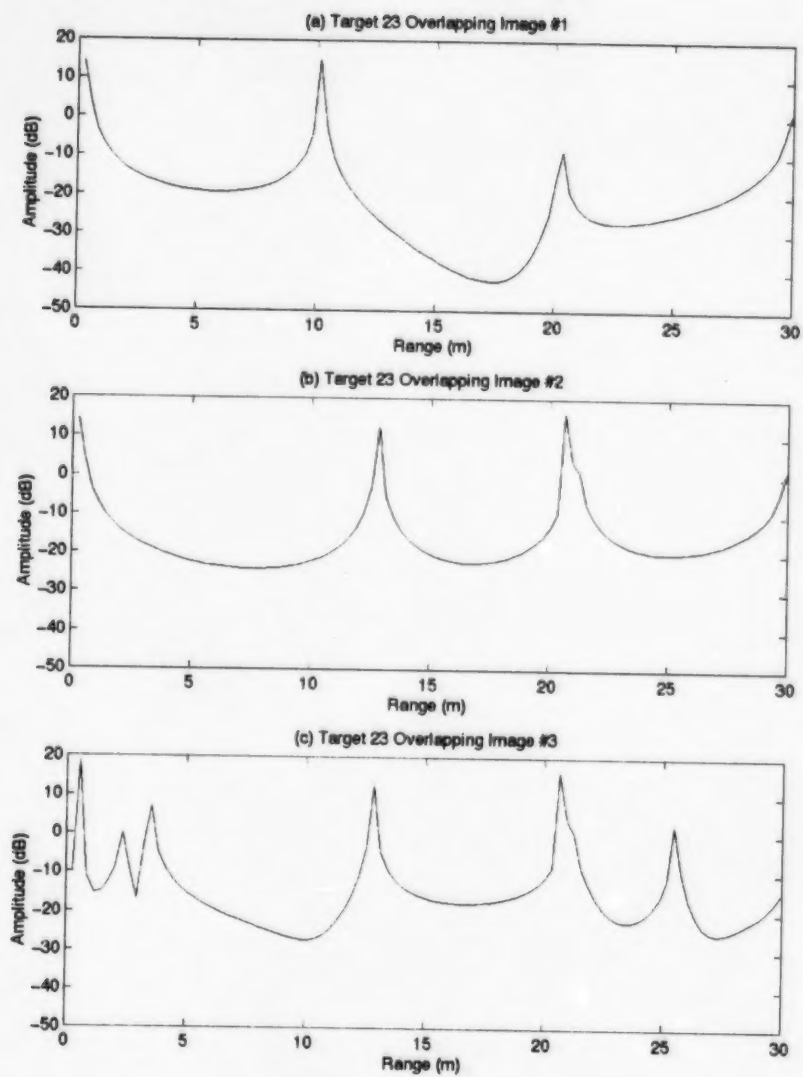
Figure 9: HRR Images for Target 5

19

Figure 10: Identification Results for Target 5

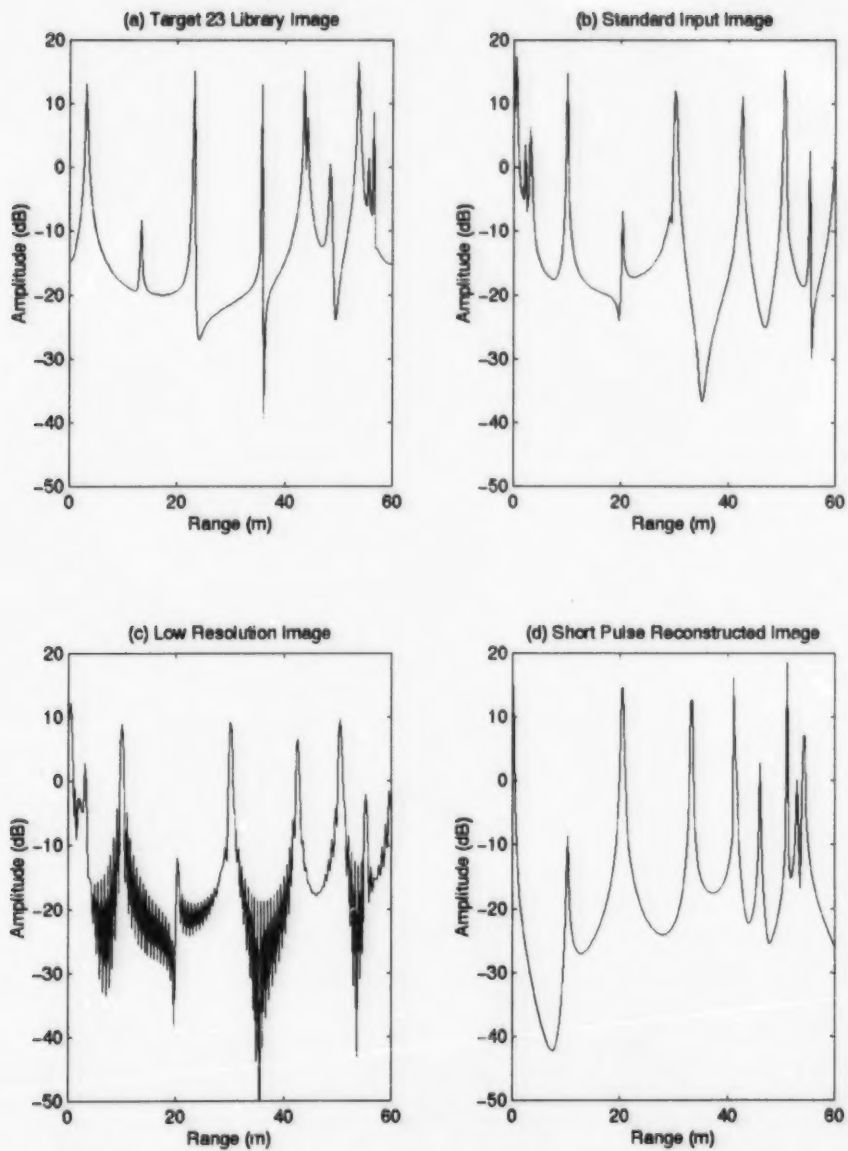**Figure 11: Overlapping Images for Target 23**

21

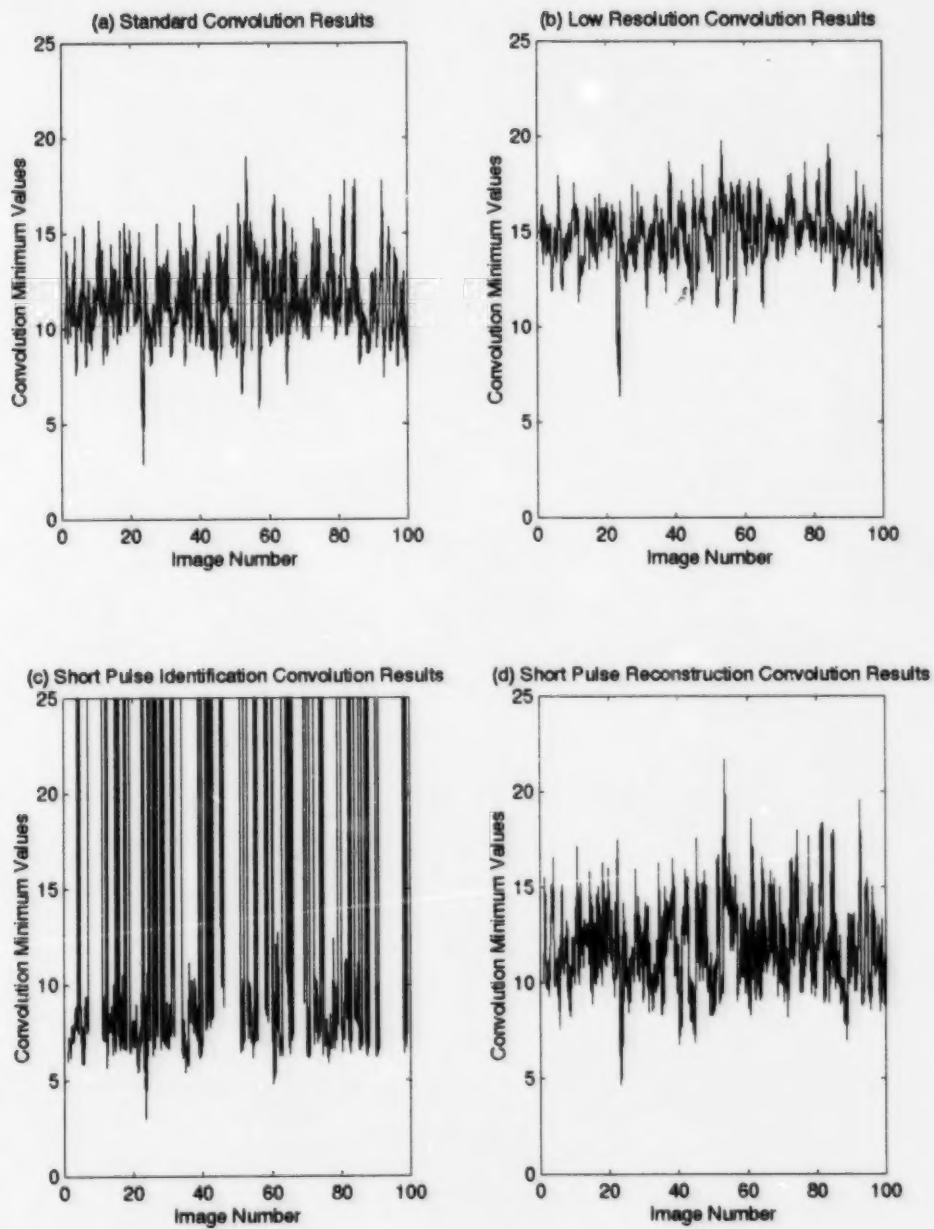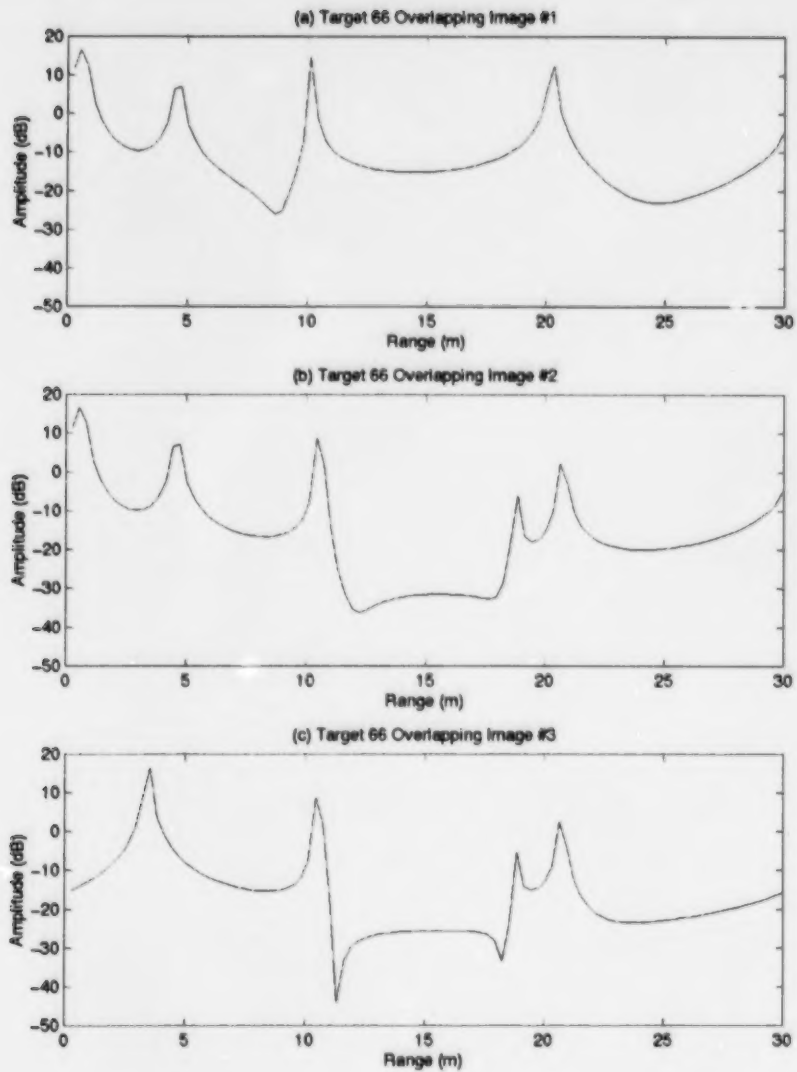**Figure 12: HRR Images for Target 23**

22

Figure 13: Identification Results for Target 23

23

Figure 14: Overlapping Images for Target 66
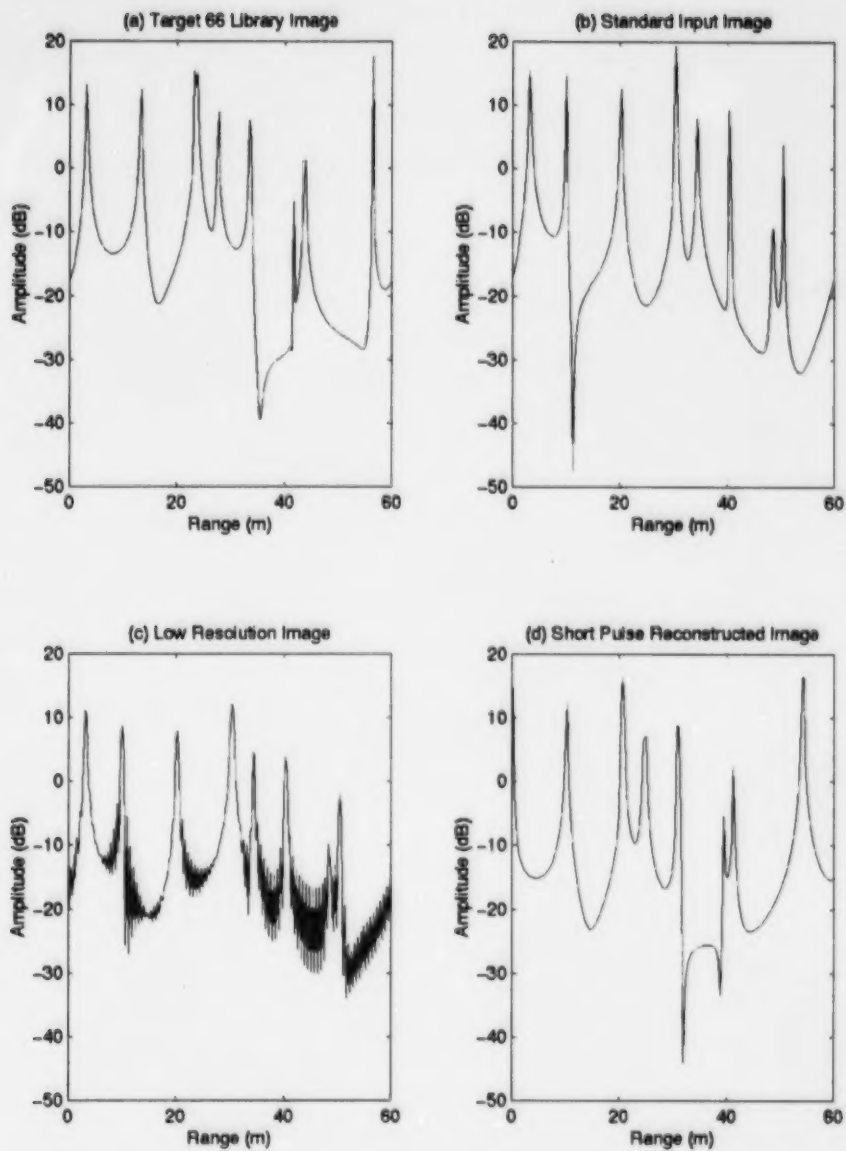
24
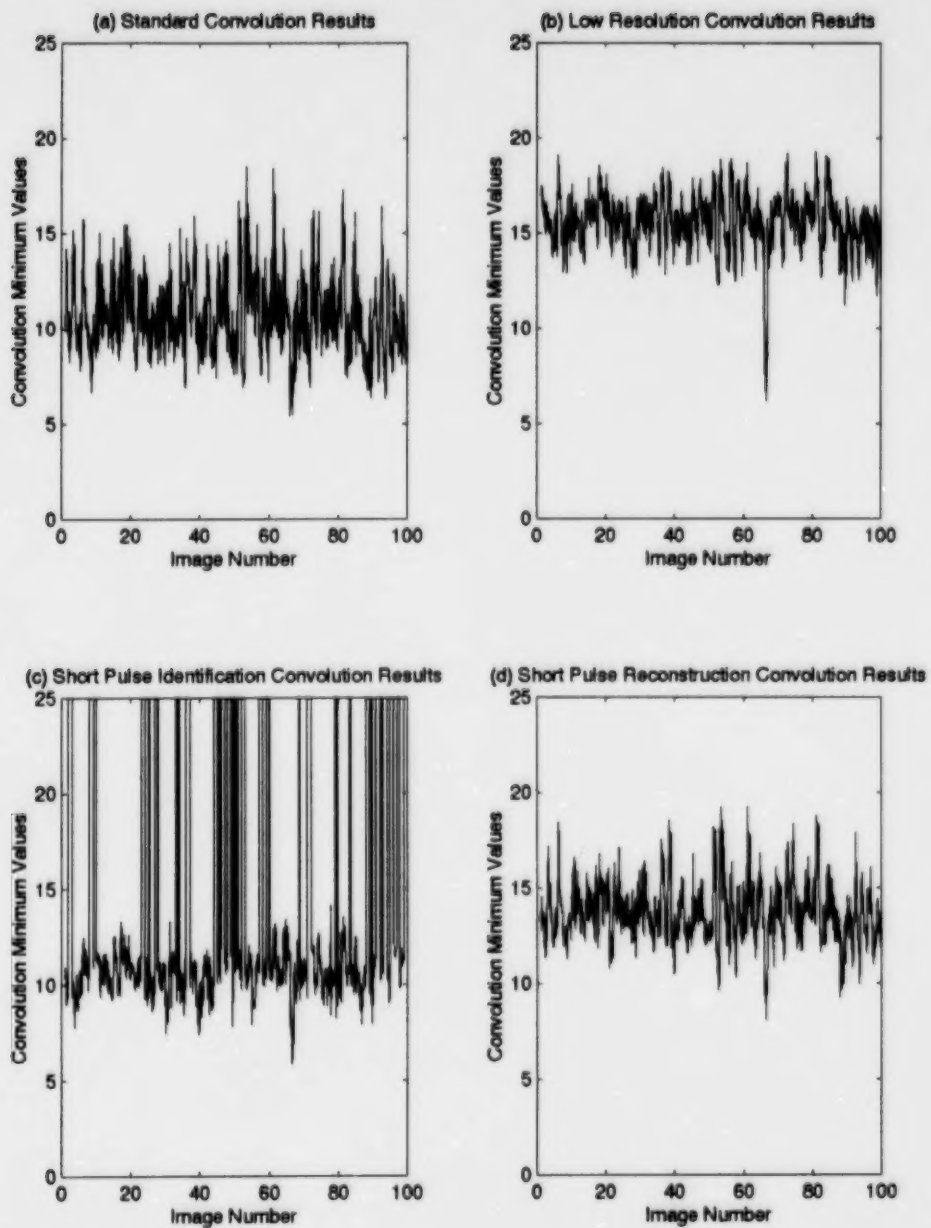
Figure 15: HRR Images for Target 66

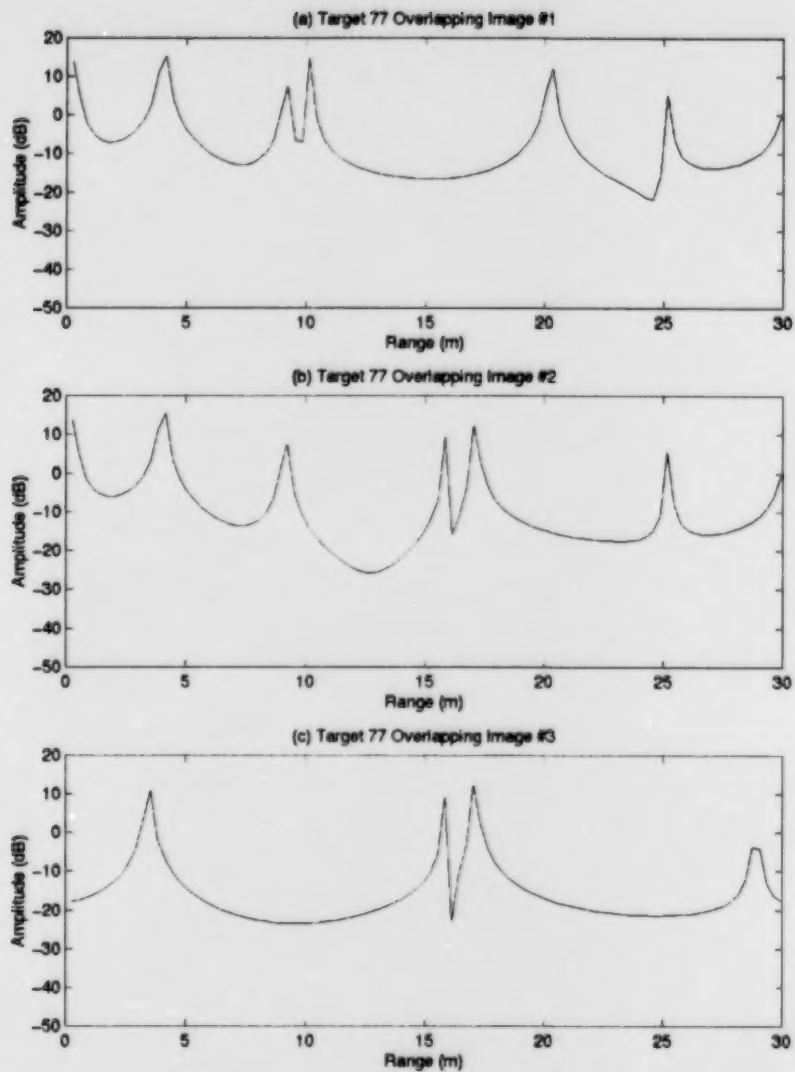**Figure 16: Identification Results for Target 66**

26

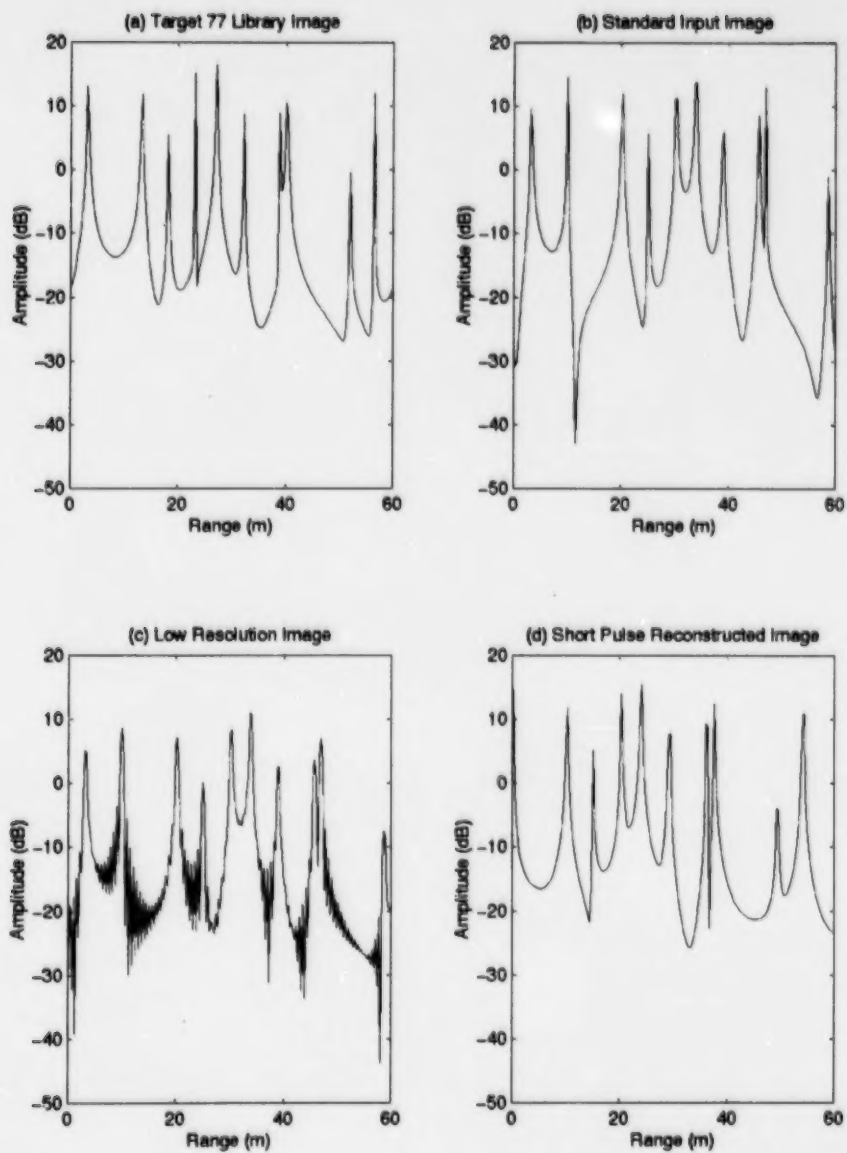**Figure 17: Overlapping Images for Target 77**
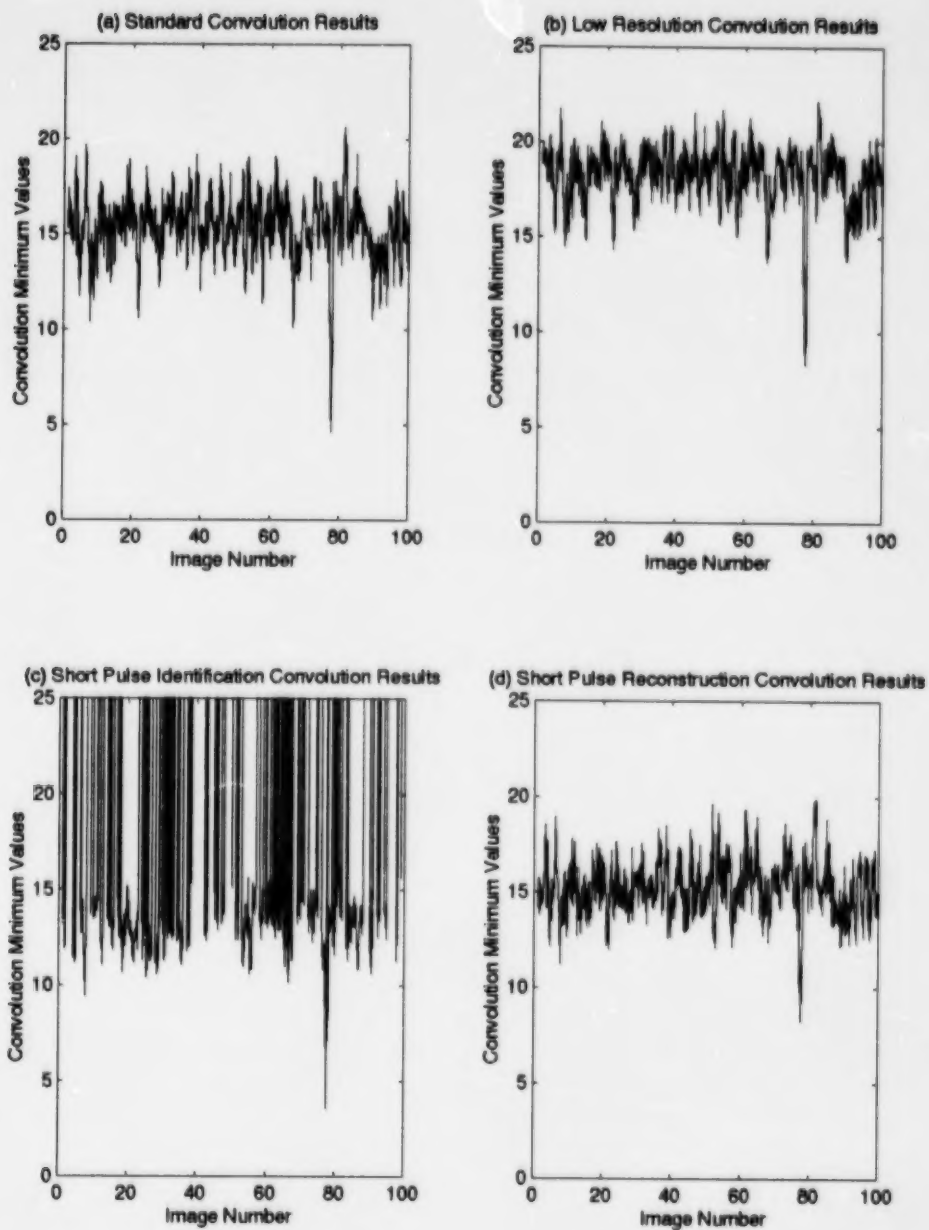
Figure 18: HRR Images for Target 77

Figure 19: Identification Results for Target 77

6.3 Velocity Tests

For these tests, the target was compensated "perfectly" for heading. The velocity compensation was 310, 320 or 330 m/s, instead of the correct target speed of 300 m/s. Table 3 shows the results. The darkened areas indicate a failure to identify the correct target. The question marks indicate an uncertainty as to whether the SPR process succeeded or failed in reconstructing the target. This was performed using a visual comparison with the conventional image. As expected the SPR method performed better than the conventional method. The shorter time to collect the signatures in the presence of imperfect compensation gives the SPR method the advantage here. Imperfect compensation leads to multiple peaks appearing in the HRR signature. For these examples, twice the time is required by the conventional technique over the short pulse techniques to collect the complete waveform, thus leading to greater errors in the motion compensation, causing more peaks in the HRR images. Algorithms could be added to correct for the multiple peak phenomena, but these will not be easy to implement in real time as some targets images may have closely spaced peaks at some aspect angles. Figure 20 shows the degradation of the HRR image for target 5 with respect to poorer compensation for the conventional HRR processing. Parts b, d, f, and h show multiple peaks and general spreading as the compensation gets worse. Parts c, e, g, and i show a general rise in the identification results, with the wrong target being selected for 20 m/s and 30 m/s error in target velocity. A similar figure for target 23 is shown in Figure 21 for SPR. While b, d, f, and h show degradation, it is not as dramatic as the conventional HRR process. The SPR technique breaks down at 30 m/s here.

Velocity (m/s)	Target	Conventional	SPR results	SPR Redraw	SPI Results	Low Resolution
310	5	5/29.6	5/29.6	yes	5/31	5/30.8
310	23	23/30.6	23/29.6	yes	23/30	23/30.6
310	66	66/29.8	66/30	yes	66/30.8	66/30.4
310	77	77/30.6	77/29.6	yes	77/30.2	77/30.6
320	5	61/30.4	5/29.6	yes	none	5/29.6
320	23	23/30.6	23/30.6	no ?	none	23/30.6
320	66	66/29.8	66/29.8	yes	28/31	66/29.8
320	77	77/30.6	77/30.6	yes	53/30.6	77/30.6
330	5	61/30.4	5/29.6	yes	none	5/29.6
330	23	92/30.4	92/30.4	yes ?	none	23/30.6
330	66	92/30.6	66/29.8	yes	92/31 (none)	66/29.8
330	77	92/30.4	92/30.4	yes	none	77/30.6

Table 3: Velocity Compensation results

The low resolution HRR method performed the best of all the algorithms here. In all subsequent tests this performs the best as well. The advantage of not sorting multiple images and reduced dwell time give it the advantage for the library used here. While the results using this library may not reflect a fair comparison between the SPR, SPI and low resolution HRR algorithms, they do indicate that setting the range resolution requirements for attaining good target identification performance will require some thought. Would larger targets require the same resolution constraints that the smaller targets have? On larger targets the major scattering points would be spread out, requiring lower resolution to extract these features. But, larger targets have the capability to carry more external hardware, which would require higher resolution to extract these features. The best selection for resolution for larger targets can not be made arbitrarily. In [4], Van Der Heiden discusses optimisation of range resolution with respect to target classification.

The SPI method performed the worst here. The prime reason is due to the constraint of counting the number of peaks above a threshold. If the total number of peaks in either of the small images is greater than the number of peaks in the library image, then that target is eliminated as a possible target. As can be seen in Figure 22, the imperfect compensation results in multiple peaks forming where there should be single peaks. Since all peaks above a threshold are counted, this results in a large rejection ratio. This problem may be alleviated by using an algorithm that determines if the range profile is properly focussed. This would not be a simple task to perform, as the algorithm would have to compensate for multiple target motions, each producing their own de-focussing. There are velocity tolerant HRR stepped frequency waveforms available that can alleviate this problem [4]. This involves using a staggered PRF, where the time between each pulse is set so that HRR images are focussed for any velocity.
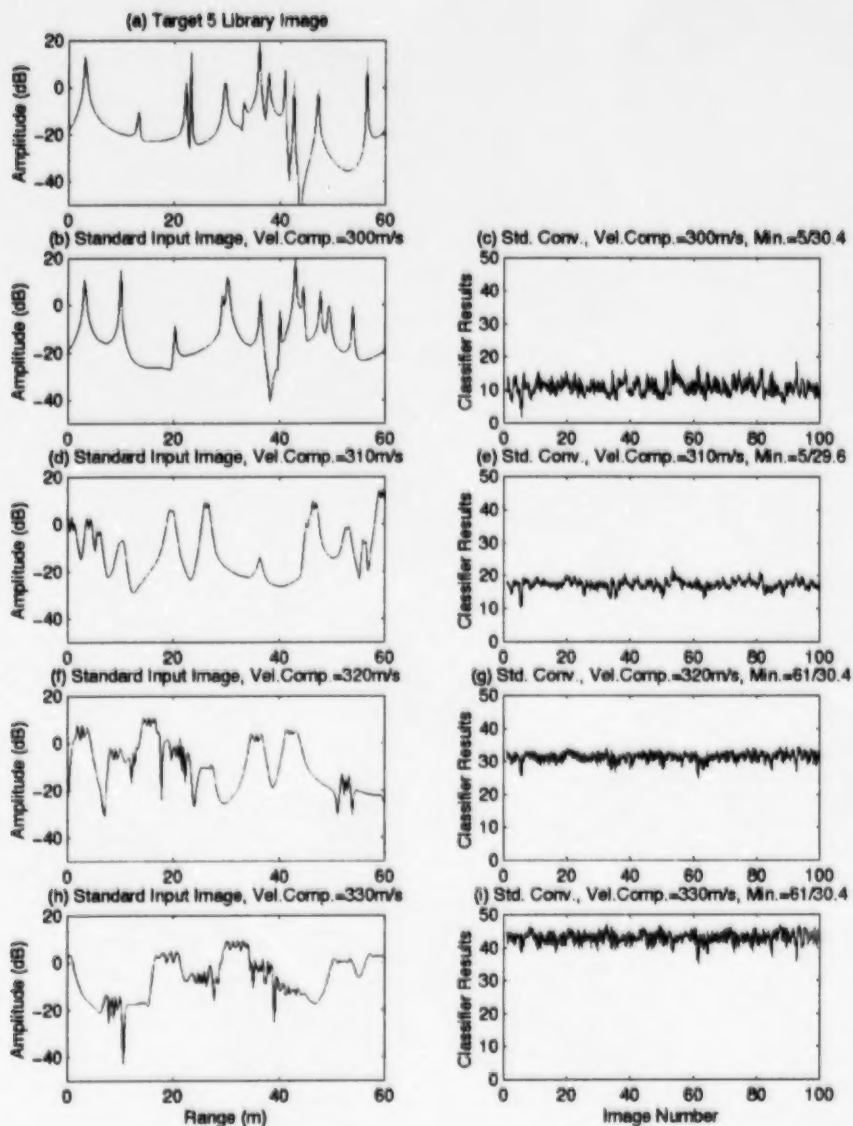
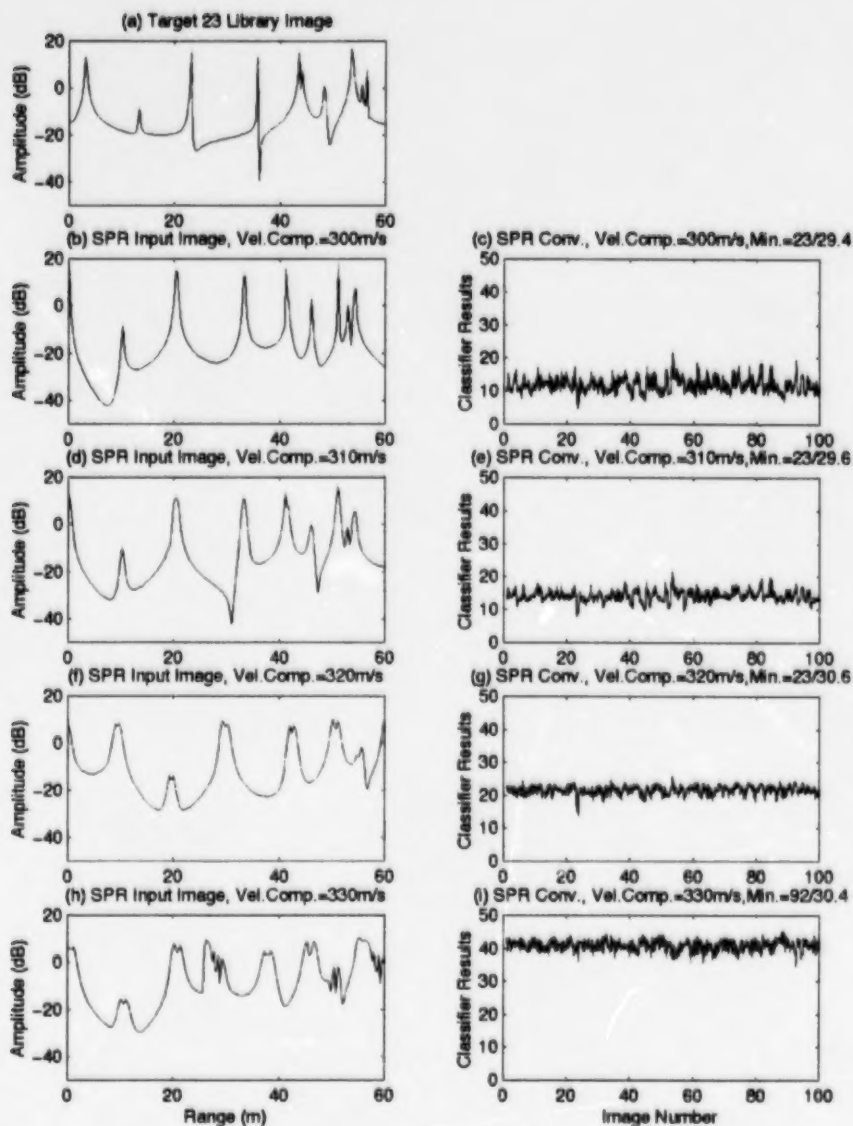**Figure 20: Velocity Compensation Error Test, Conventional HRR**

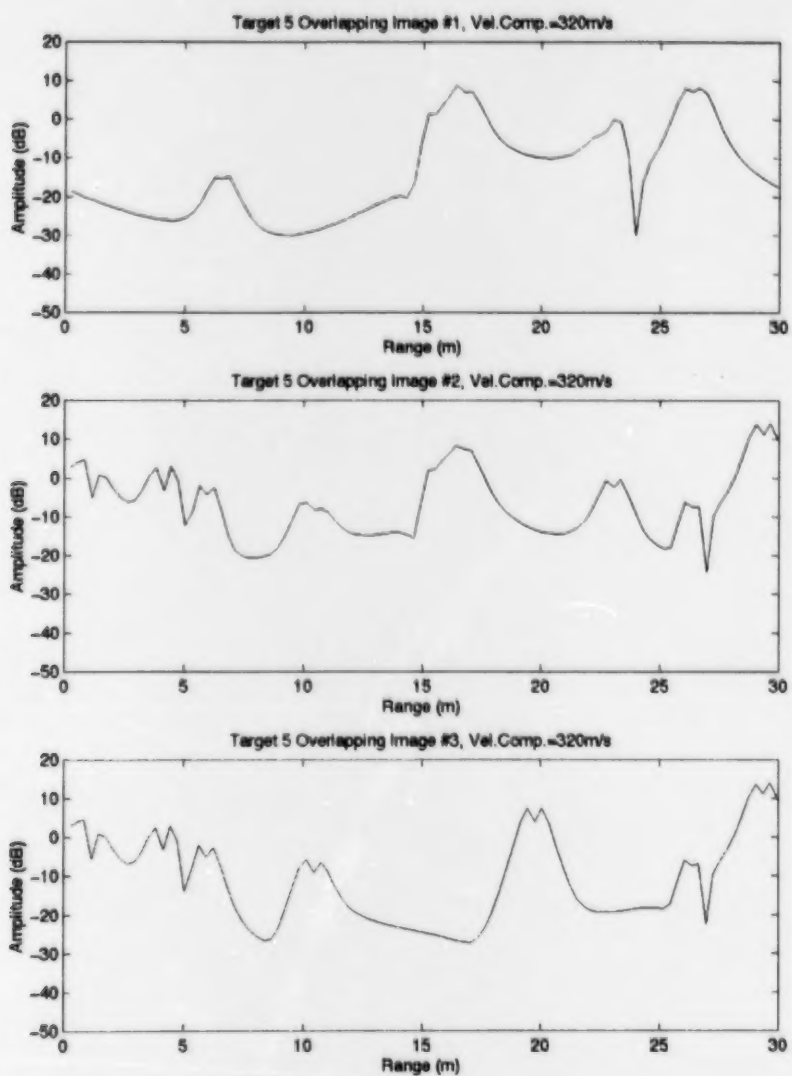**Figure 21: Velocity Compensation Error Test, SPR Method**

Figure 22: Effect of Velocity Mismatch

6.4 Heading Tests

Heading compensation errors of +/-1° were tested with interesting results. As can be seen in Table 4, only one identification failure occurred. This was in the SPR routine for target 5 at 31° heading. Figures 23 shows the reconstructed target 5 and corresponding SPR results for headings of 29°, 30° and 31°. As can be seen in Part (f) of Figure 23, the reconstruction of the target was performed correctly. However, as shown in Part (g) of Figure 23, target 88 was selected as the most likely target, although not by a large margin. A second interesting result occurred with the SPR routine for target 23 at 31° heading. Figures 24 shows the reconstructed target 23 and corresponding SPR results for headings of 29°, 30° and 31°. While the reconstruction of the target was not successful, as can be seen in Part (f) of Figure 24, the identification algorithm still selected the correct target. The reason for the success is that some of the larger scatterers are put in the correct order by the algorithm. These results emphasize the affect of aspect angle on the SPR process. The SPI process has no problem with heading in these cases.

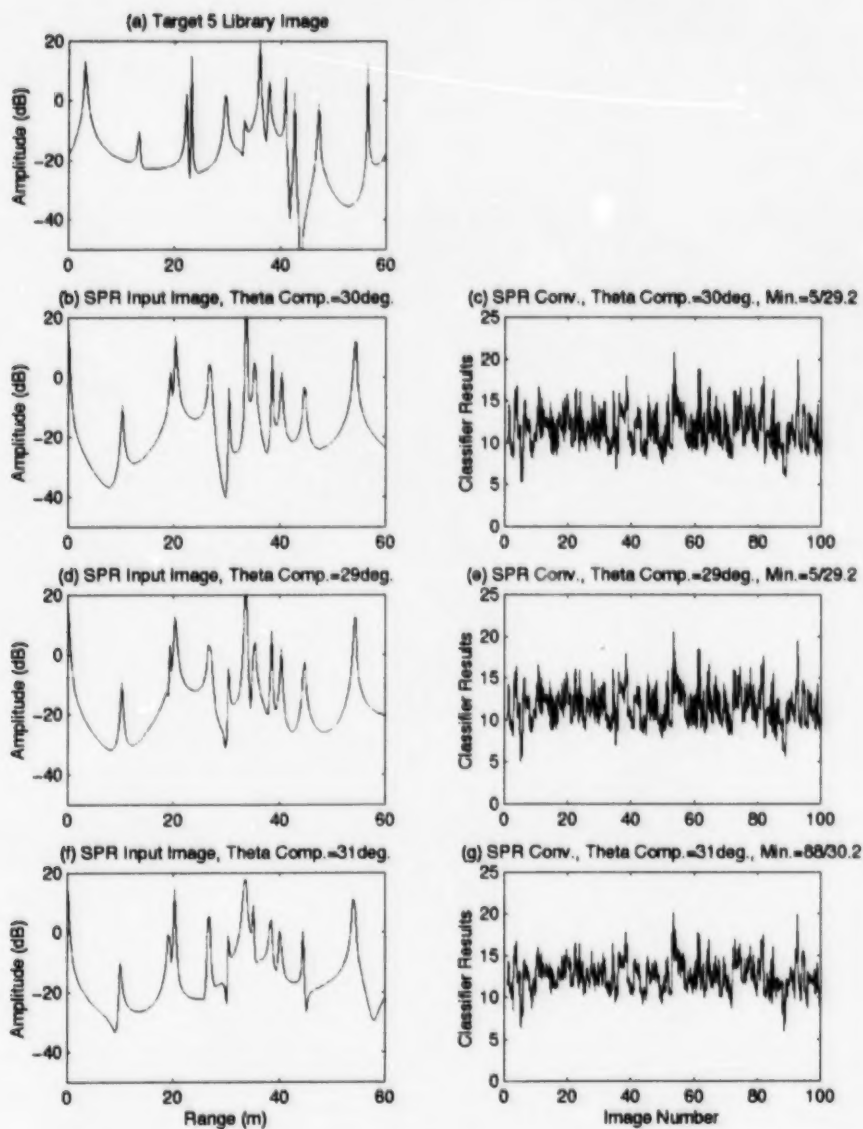| Angle	Target	Conventional	SPR results	SPR Redraw	SPI Results	Low Resolution
29°	5	5/30.4	5/29.2	yes	5/30.2	5/30.8
29°	23	23/30.4	23/29.4	yes	23/31	23/30.6
29°	66	66/30.2	66/30	yes	66/30.8	66/29.8
29°	77	77/30.2	77/30.2	yes	77/30.2	77/30.8
31°	5	5/30.4	88/30.2	yes	5/30.6	5/30.8
31°	23	23/30.2	23/29.4	no	23/30.4	23/30.6
31°	66	66/30	66/29.2	yes	66/30.8	66/30.4
31°	77	77/30	77/30.2	yes	77/30.8	77/30.8

Table 4: Heading Compensation Results

Figure 23: Heading Compensation Error Test, Target 5, SPR Method
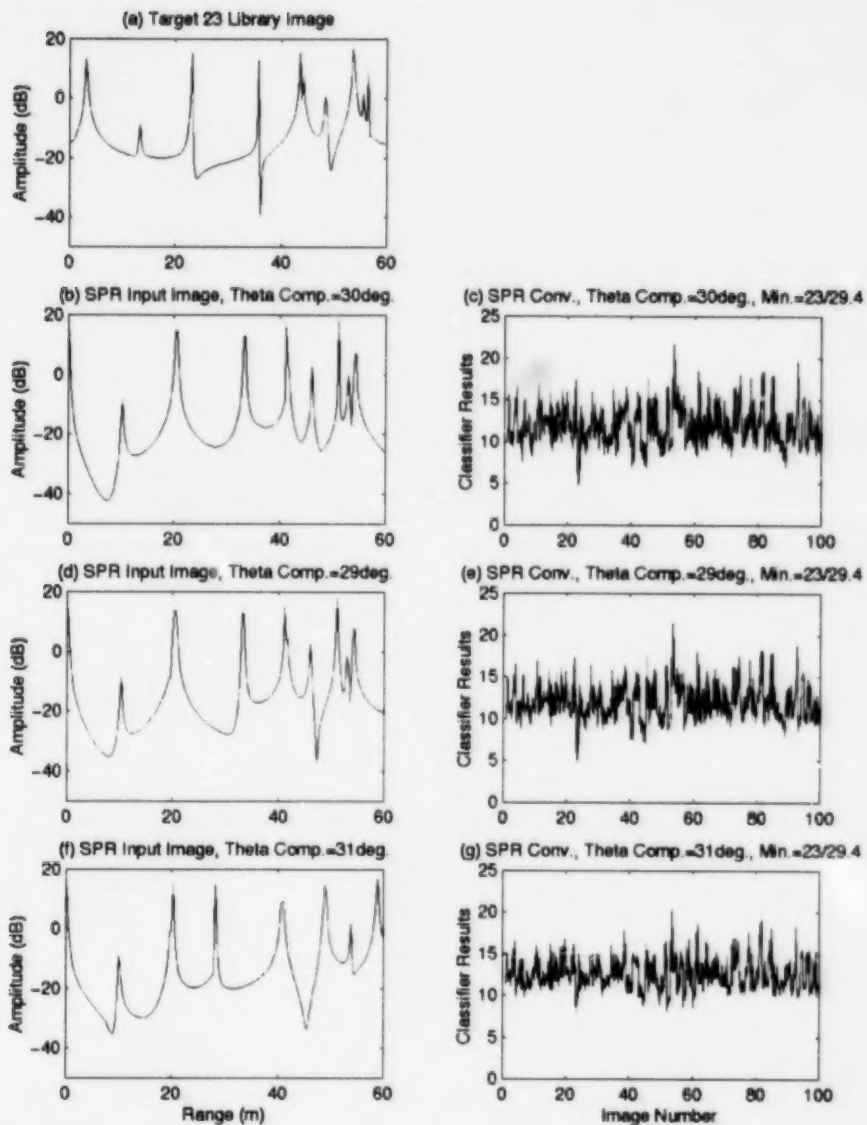
Figure 24: Heading Compensation Error Test, Target 23, SPR Method

37

6.5 Acceleration Tests

Table 5 shows the overall performance of each algorithm for increasing target acceleration. The SPI and the low resolution routines were able to identify all of the targets correctly. The conventional method degraded with increase in target acceleration. Figure 25 shows a similar degradation to that of the velocity plots in Figure 20. As shown in Figure 26, the SPR routine had problems with target 23 for this study. For each of the accelerations, it failed to redraw the target correctly, thus causing the identification process to fail. All the other identifiers had no problem with target 23. This is a good example of the edge effect problem for the overlapping images. It led to a readjustment of the algorithm to process the experimental data in the upcoming sections.

Acceleration (m/s^2)	Target	Conventional	SPR results	SPR Redraw	SPI Results	Low Resolution
10	5	5/29.6	5/29.6	yes	5/31	5/30.8
10	23	23/30.6	44/30.8	no	23/29.8	23/30.6
10	66	66/29.8	88/30.8	yes	66/30	66/29.8
10	77	77/30.8	77/29.6	yes	77/29.8	77/30.8
20	5	61/30.4	5/29.6	yes	5/29.6	5/29.6
20	23	23/30.6	4/30.8	no	23/30.6	23/30.6
20	66	66/29.8	66/29	yes	66/29	66/29.8
20	77	77/30.6	77/30.2	yes	77/30.8	77/30.4
30	5	92/30.4	5/29.6	yes	5/29.6	5/29.6
30	23	23/30.6	31/30.4	no	23/30.6	23/30.6
30	66	92/30.4	66/29.8	yes	66/30.8	66/29.8
30	77	92/30.4	77/30.4	yes	77/30.2	77/30.6

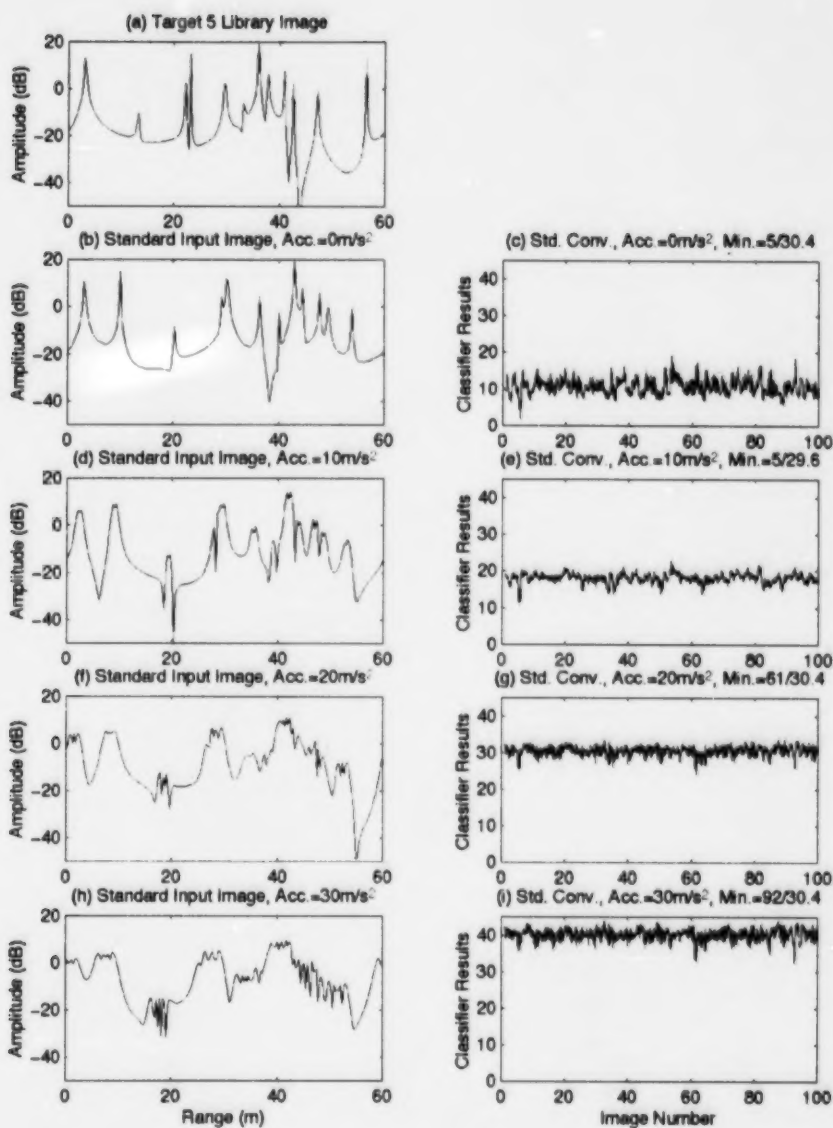**Table 5: Acceleration Compensation results**

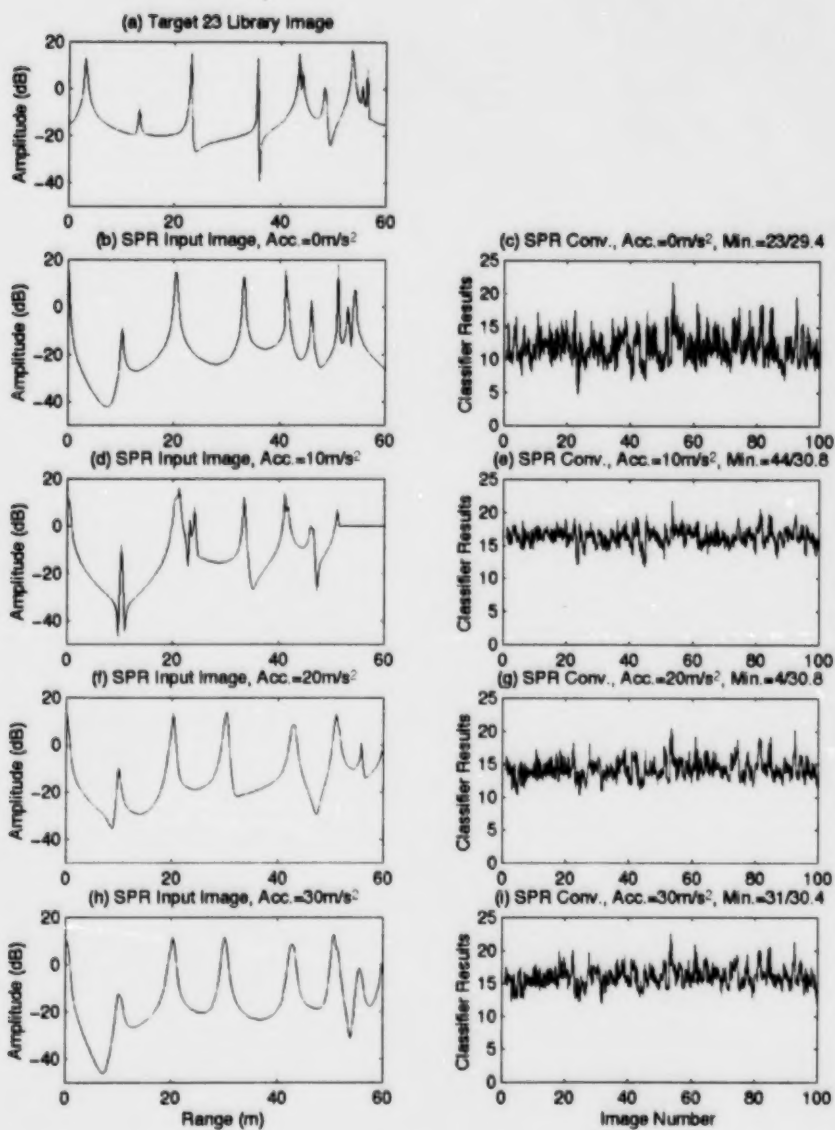Figure 25: Acceleration Error Test, Target 5, Conventional HRR

Figure 26: Acceleration Error Test, Target 23, SPR Method

6.6 Signal to Noise Ratio Tests

The SNR was varied from -20 dB to +10 dB with respect to the frequency domain signals. By performing the inverse FFT, this results in an integration in proportion to the number of frequencies used. The signal to noise ratio (SNR), as expected, reduced the SPR and SPI identification performance more quickly than the conventional approach. Surprisingly, the low resolution HRR approach had a similar performance to the conventional approach. The most likely reason for this is the 10 dB steps taken for testing SNR. The loss in SNR by using the low resolution approach, is the integration loss or 3 dB. In this case, all algorithms failed at -20 dB SNR. Figure 27 shows the degradation in the image and identification results with respect to decreasing SNR for target 66 with the conventional HRR. The degradation occurs more quickly for the SPR routine, as shown in Figure 28.

SNR (dB)	Target	Conventional	SPR results	SPR Redraw	SPI Results	Low Resolution
-20	5	53/30.2	84/30.8	no	none	64/30.6
-20	23	61/30.4	84/30.8	no	none	64/30.6
-20	66	53/30.2	72/30.8	no	none	61/30.4
-20	77	53/30.2	84/30.8	no	none	53/29
-10	5	5/30.4	5/29.8	yes	none	5/29.6
-10	23	23/30.6	12/31	no	none	23/30.6
-10	66	66/30.8	3/29.6	no	none	66/30.4
-10	77	77/30.6	77/30.2	no	none	77/30.6
0	5	5/30.4	5/29.2	yes	5/30.4	5/30.6
0	23	23/30.4	23/29.4	yes	23/30.2	23/30.6
0	66	66/30.8	66/30.2	yes	66/30.2	66/30.4
0	77	77/30.4	77/30.2	yes	77/30.2	77/30.6
10	5	5/30.4	5/29.2	yes	5/30.4	5/30.6
10	23	23/30.4	23/29.4	yes	23/30.2	23/30.6
10	66	66/30.6	66/30.2	yes	66/30.2	66/30.4
10	77	77/30.4	77/30.2	yes	77/30.2	77/30.6

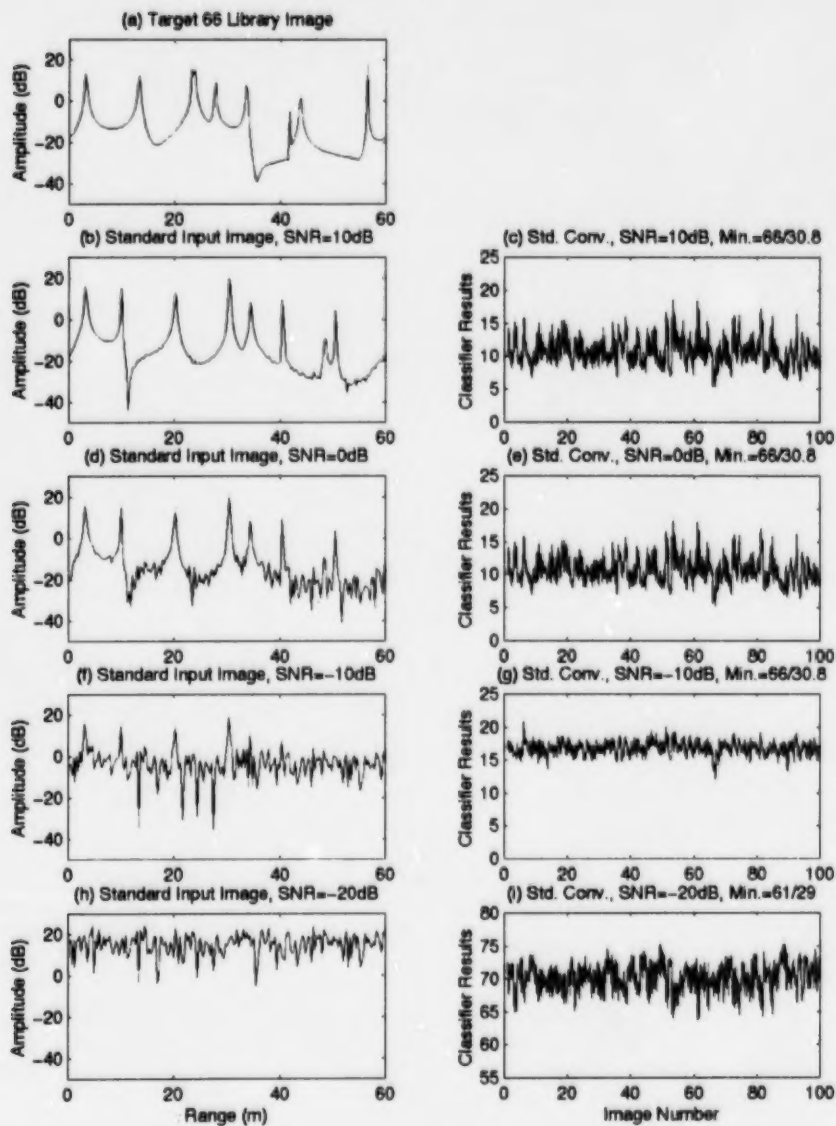**Table 6: SNR Identification Results**

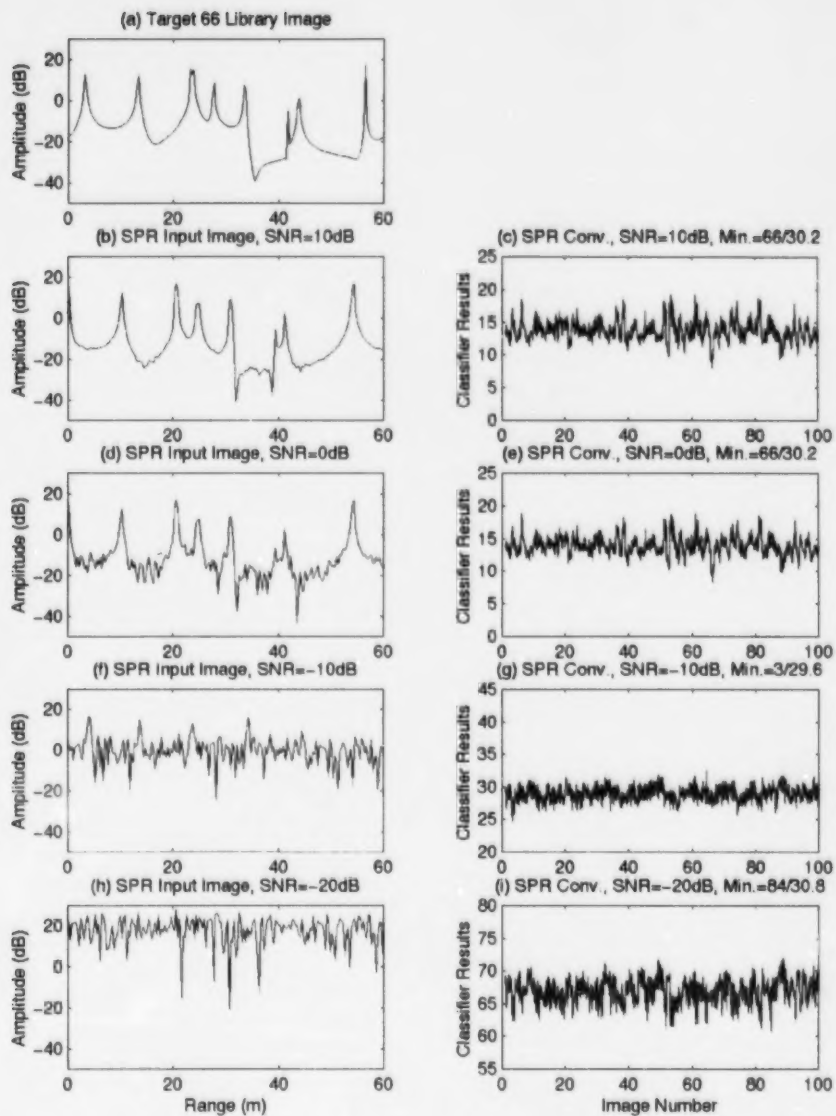**Figure 27: SNR Test, Target 66, Conventional HRR**

42

Figure 28: SNR Test, Target 66, SPR Method

43

7.0 EXPERIMENTAL TESTING OF THE SHORT PULSE RECONSTRUCTION PROCESS

Testing of the SPR technique involved setting up scenarios of corner reflector targets in known geometries, and seeing if the automatic SPR process shows the location of the individual reflectors. The Experimental Array Radar System (EARS), shown in Figure 29, was used to collect HRR data for testing the short pulse reconstruction technique. This system was developed at DREO to test adaptive nulling techniques, but it can collect radar data at multiple ranges for each pulse. The system did not have pulse to pulse frequency agility at the time of the experiments; therefore, experiments had to be performed on stationary targets. Finally, only one channel of EARS was required for the technique. EARS comprises several major subsystems; the transmitting and receiving antennas, the transmitter, A/D conversion, the data logger/control system. EARS uses a high aspect ratio parabolic antenna for transmission and two arrays for reception. EARS is horizontally polarized and the receiver system forms an inverted "T". An
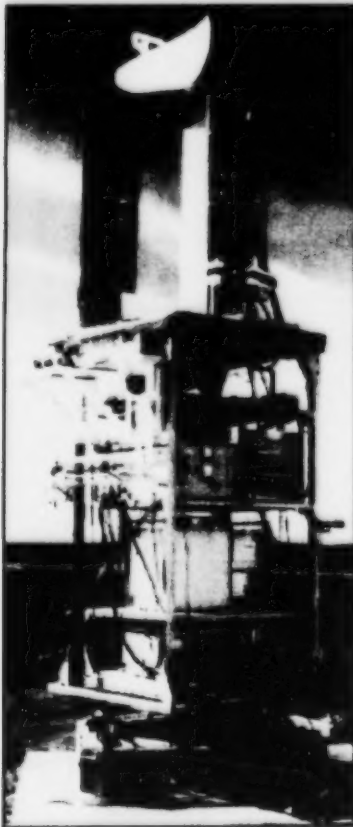
eight element vertical array fed from a 1.4 by .6 meter parabolic reflector is used as the main receive antenna. Each element has 25 dB gain with a 4.5 degree azimuth beamwidth and a 17 degree elevation beamwidth. The vertical spacing between elements is 12.5 cm. An eight element horizontal array is used as the sidelobe canceller for the main array. This was not required for the trials. A Travelling Wave Tube Amplifier (TWTA) is used for coherent transmission of RF signals. The agile frequency range of the TWTA is from 8.9 to 9.4 GHz with a 5 MHz bandwidth. The TWTA has a peak power of 8 KW. The data was collected across the 500 MHz bandwidth with a 5 MHz step size with a pulse width of 200 ns.

High Speed Analog to Digital conversion is performed on the 16 channels from EARS. These A/D's perform 12 bit sampling up to a rate of 20 MHz. The boards have a built in RAM that can store up to 256 K of 12 bit data. Once the RAM is filled the data is down loaded to the VME-based control and data logger system. The system controls EARS functions and logs data from the A/D converters at a 20 MHz rate. The storage device used is a disk array capable of storing 10 Gbytes of data. Once a trial is performed, data can be transferred to an Exabyte tape unit for off-line analysis.

Figure 29: Experimental Array Radar System

The high sampling rate gives EARS a capability of performing sampling at the intermediate frequency. Using this method reduces the number of A/D's required by one half and eliminates I and Q channel mismatch found in conventional systems. The short pulse reconstruction technique takes advantage of EARS capability of sampling overlapping range cells in one pulse.

The system was installed near the Ottawa River. The HRR experiments were performed when the river was frozen over.

The EARS data consisted of 101 files collected for a period of 5 seconds each across the frequency band of 8.9 to 9.4 GHz for a range of 1200 to 2200 meters with a pulse width of 200 ns. To convert the data to single frequency input the 50 pulses of data were first extracted from tape and down loaded to an ASCII file. The data was collected at a 20 MHz sampling rate per pulse, resulting in 7.5 meters between each sample or 132 range cells. The phase of the data was generated using a Hilbert transform and a low pass filter to reduce the number of range cells to 66 or 15 meters between each sample. The fifty samples were averaged to increase the signal to noise ratio of the data. This was performed at each frequency resulting in 66 frequency profiles corresponding to each range. An inverse FFT is then performed on each range bin resulting in 66 HRR images in 15 meter increments. The experimental configurations had a vertical length of over 30 meters. The 200 ns pulsewidth would only cover 30 meters. By taking multiple overlapping HRR images, one should be able to recreate the full image using the SPR sorting routine.

7.1 1998 HRR Experiments

The 1998 experiment used to test the short pulse reconstruction technique involved the use of six corner reflectors of equal radar cross section. The corner reflectors were triangular corner reflectors with side dimensions 0.298 m. Equation 15 is gives the maximum theoretical radar cross section (in dB) of these corner reflectors.

$$RCS_{dB} = 10 \, LOG_{10} \left[\frac{3\pi \, d^4}{\lambda^2} \right] \tag{15}$$

The variable λ is the wavelength of the radar signal. From Equation 14, their cross-section at 9 GHz is 18.25 dB.

There were ten HRR measurements performed in 1998. The first six tested the range resolution of EARS and were not related to the SPR experiment. The first experiment specifically for SPR was measurement 7, which was used to verify that the direction of the SPR sorting routine is correct. For this, four reflectors were placed with the following spacing: 4 m, 4m, and 11m. Figure 30 shows eight consecutive amplitude versus relative range windows from measurement 7. The amplitude versus relative range windows overlap each other by 15 meters.

The SPR routine searches for the start of the target by searching left to right, top to bottom with respect to the images. The start of the target coincides with the first peak that surpasses a selected threshold. A low threshold is set at first to catch the start of the target. Due to the pulse width of 30 meters, and the 15 meter spacing between windows, three overlapping windows will contain a particular reflector. The HRR profile of that reflector will be largest for the second overlapping peak. Since we are attempting to find the start of the configuration, we require a lower threshold for finding this. Once the start of the configuration is determined the threshold is set to a higher level to sort out the rest of the configuration. Also, once a peak's position is found, an area about that peak will not be used in subsequent images for reconstructing the HRR image. This is to avoid cases where two closely spaced reflectors could slightly alter the peak position in the HRR profile. For these measurements, this area is set to zero because the configurations were fixed in position. A normalization to the largest peak in all the images was also included to simplify setting thresholds. Figure 31 shows the reconstructed return. For this algorithm, the peak amplitudes are plotted at ranges relative to the start of the configuration. An average minimum of the images is used for determining minimum value in the plots. Note that the fourth image from the top of Figure 30 could be used as a template for target identification, but from the single image, one could not determine the start of the configuration automatically. Figure 31 demonstrates a successful automatic sorting of the targets making use of the multiple HRR images.

Figures 32 and 33 show the overlapping images and SPR results for Measurement 8, which had 9 meters spacing between each of the six reflectors, for a total target length of approximately 45 meters. The fifth image from the top of Figure 32 displays edge effect problems, where there appears to be 5 reflectors in the window. At 9 meters spacing, this would correspond to 36 meters, where the 200 ns radar pulsewidth should only enable 30 meters to be illuminated. The sorting routine is able to handle this problem by windowing out areas around identified peaks; however, investigation into the problem in the radar system is underway. The case where scatterers are exactly one pulsewidth apart would result in the rejection of one of the peaks, which is not a desirable scenario for target identification. Figure 33 shows that the sorting was successful, displaying evenly spaced targets extended across 45 m. Note that all the reflectors do not have identical strength. This is due to the nature of the experiment, where all the reflectors are mounted on tripods on the ice and were not exactly aligned. The reflectors exact RCS were not calibrated as well. The interest here was to determine the configuration's geometry.

Measurement 9 had a random spacing. For this six reflectors were placed at spacing away from EARS of 8m, 6m, 9m, 13m and 10m. The overlapping images and SPR results are displayed in Figures 34 and 35. The more complicated random spacing between the reflectors posed no problem to the SPR routine.

Measurement 10 was the next test with 11 meters spacing between each of the six reflectors. The spacing gave an extended target of 55 meters in length, which is quite near to 2 times the 30 m pulsewidth. This again was solved by the sorting algorithm, as shown in Figures 37 and 38.
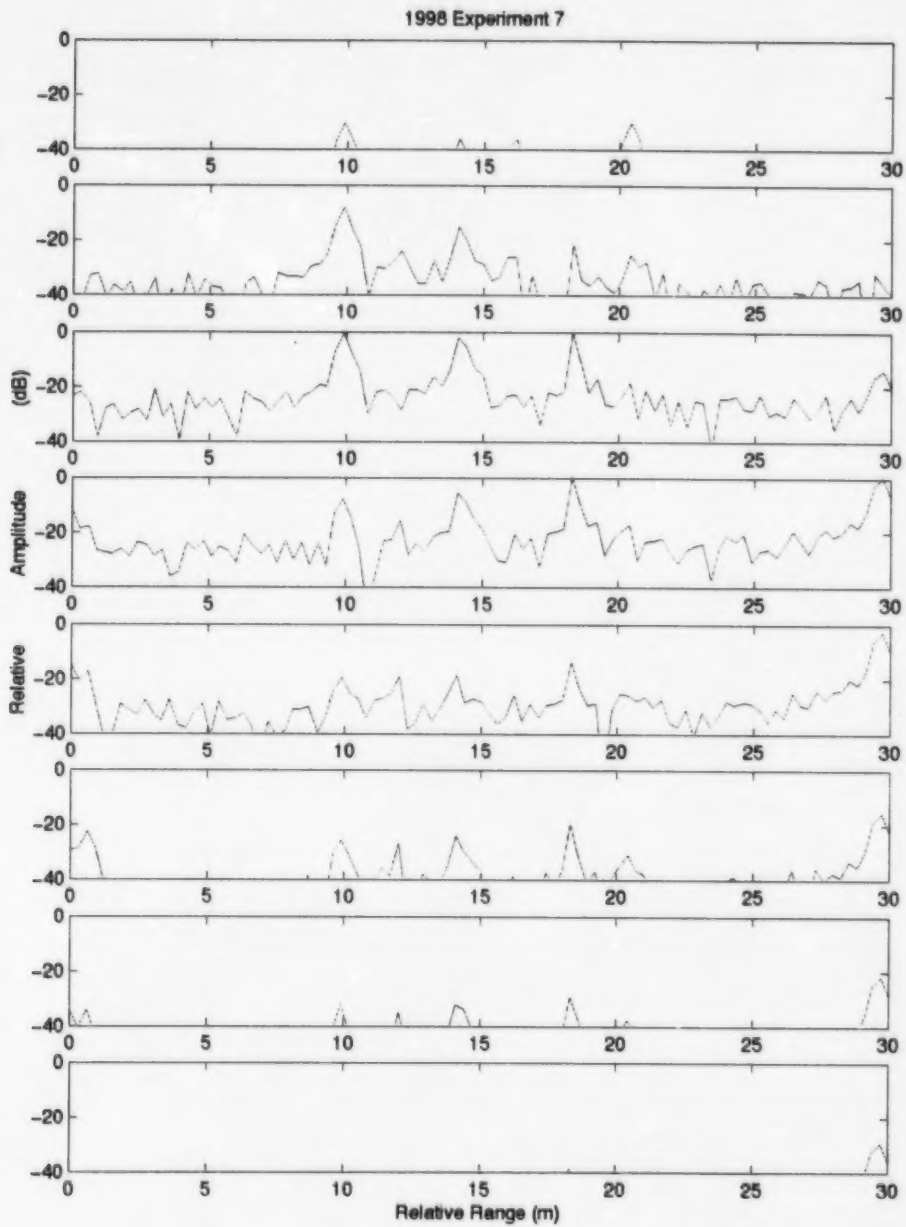
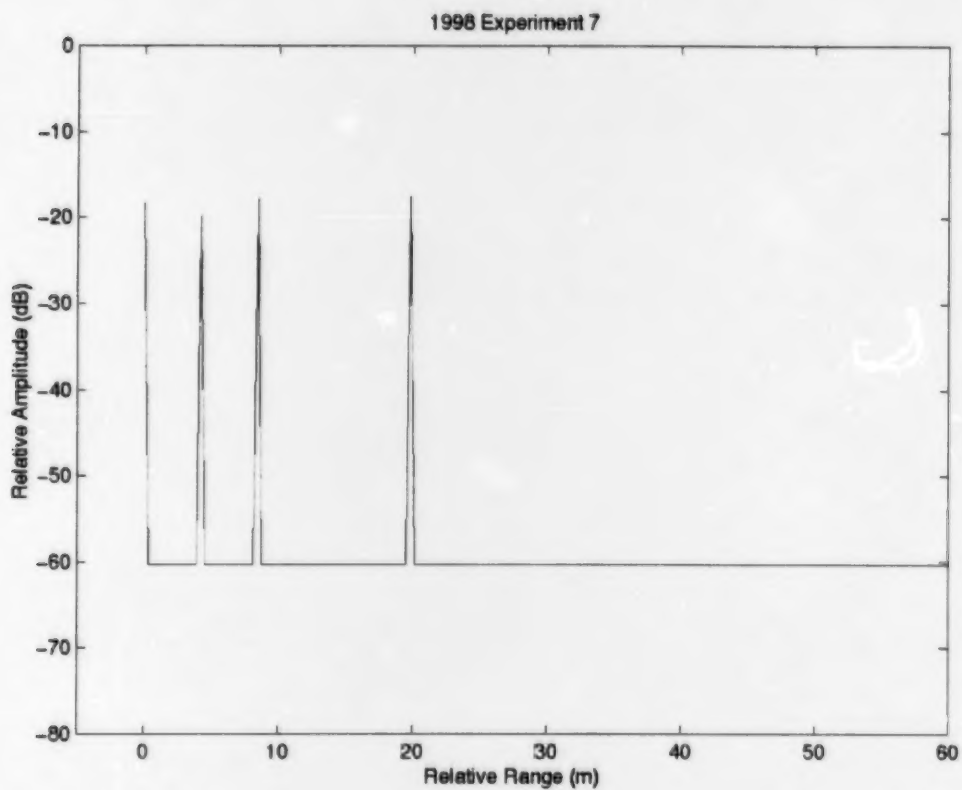**Figure 30: Overlapping Images for Measurement 7.**

47

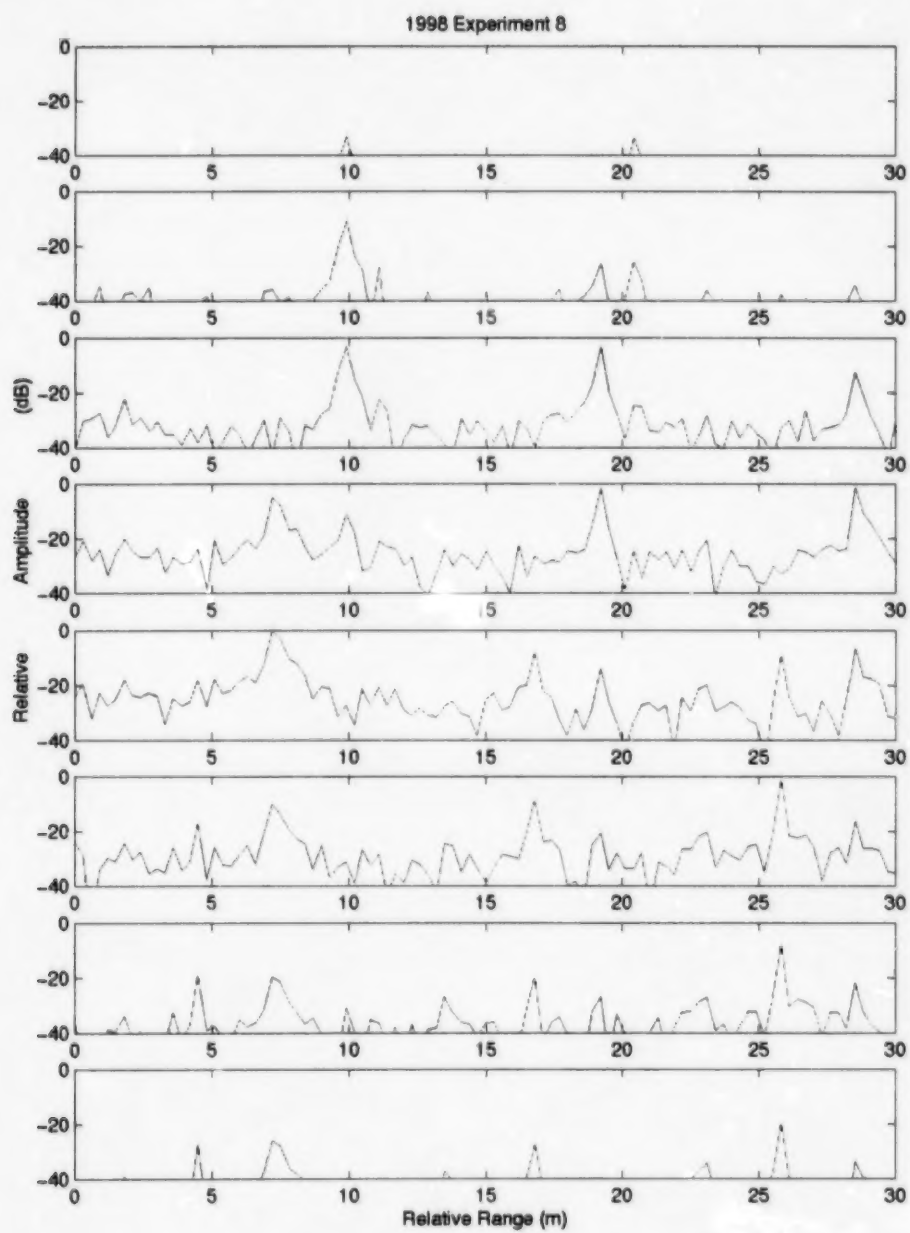Figure 31: SPR Results for Measurement 7, 4 Targets Spaced at 4, 4, 11 m Intervals
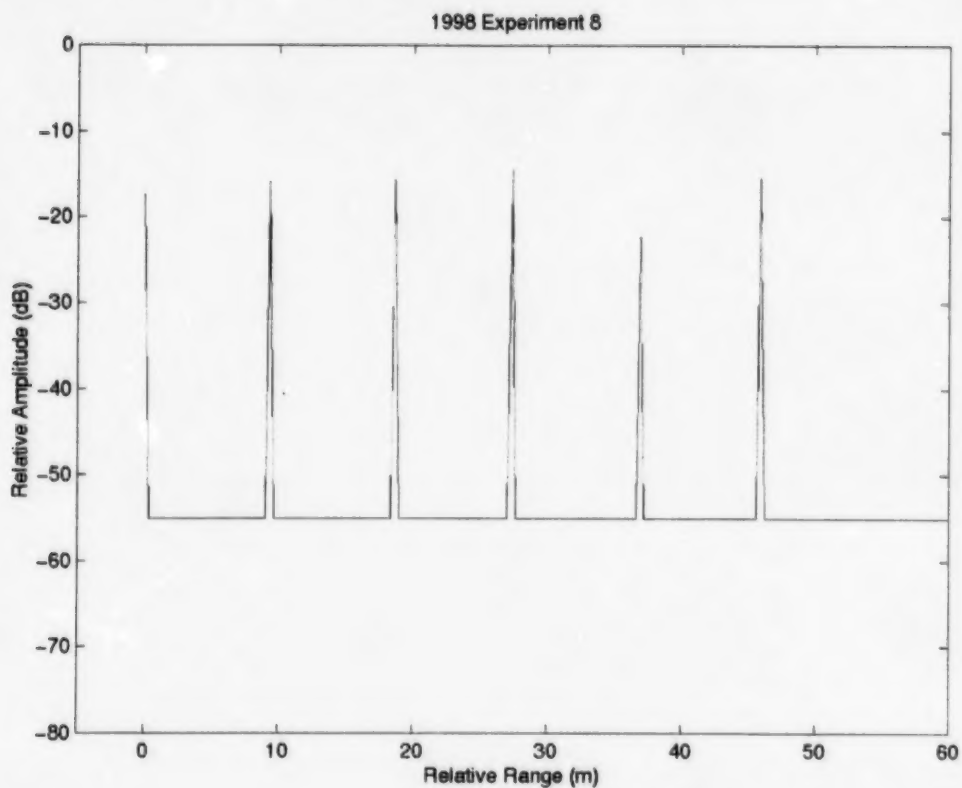
Figure 32: Overlapping Images for Measurement 8.

49

Figure 33: SPR Results for Measurement 8, 6 Targets Evenly Spaced at 9 m Intervals
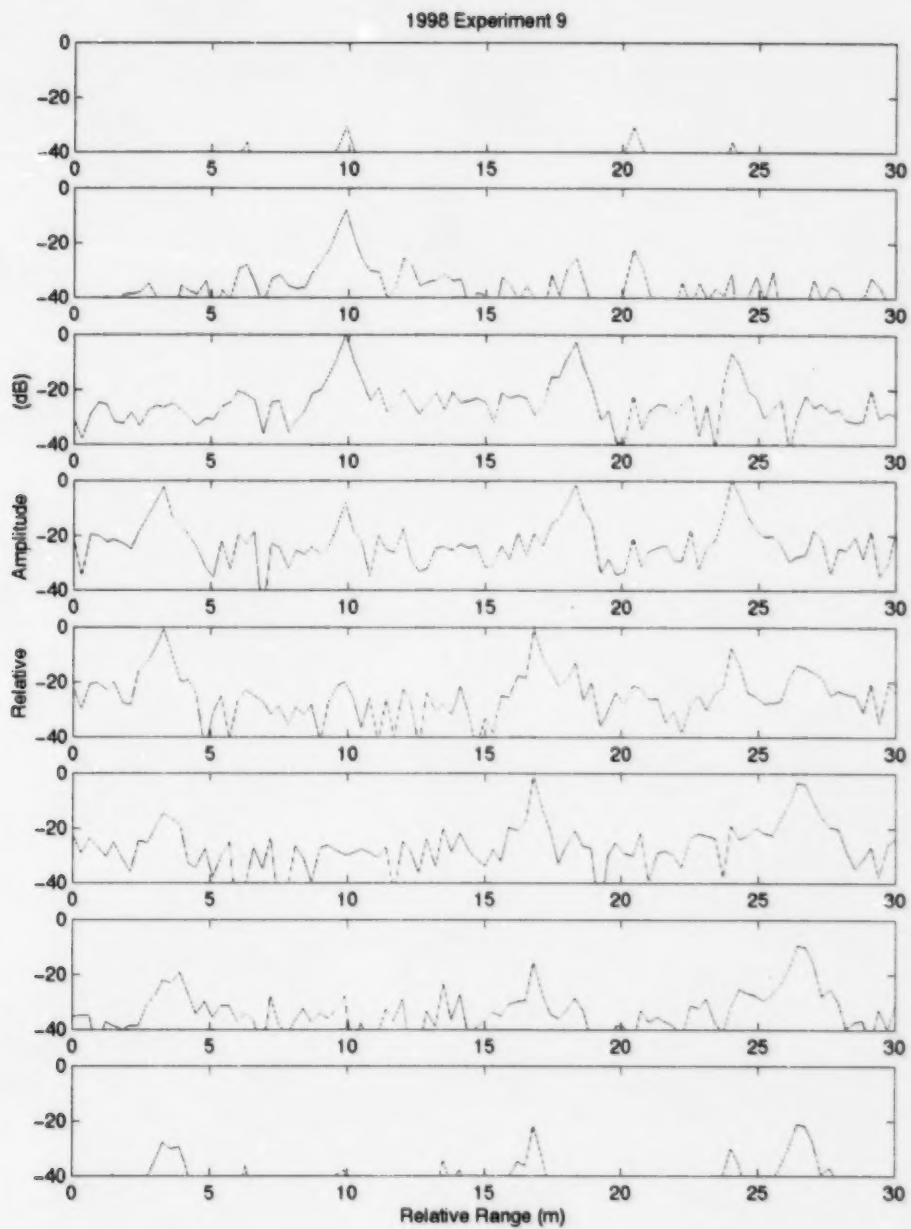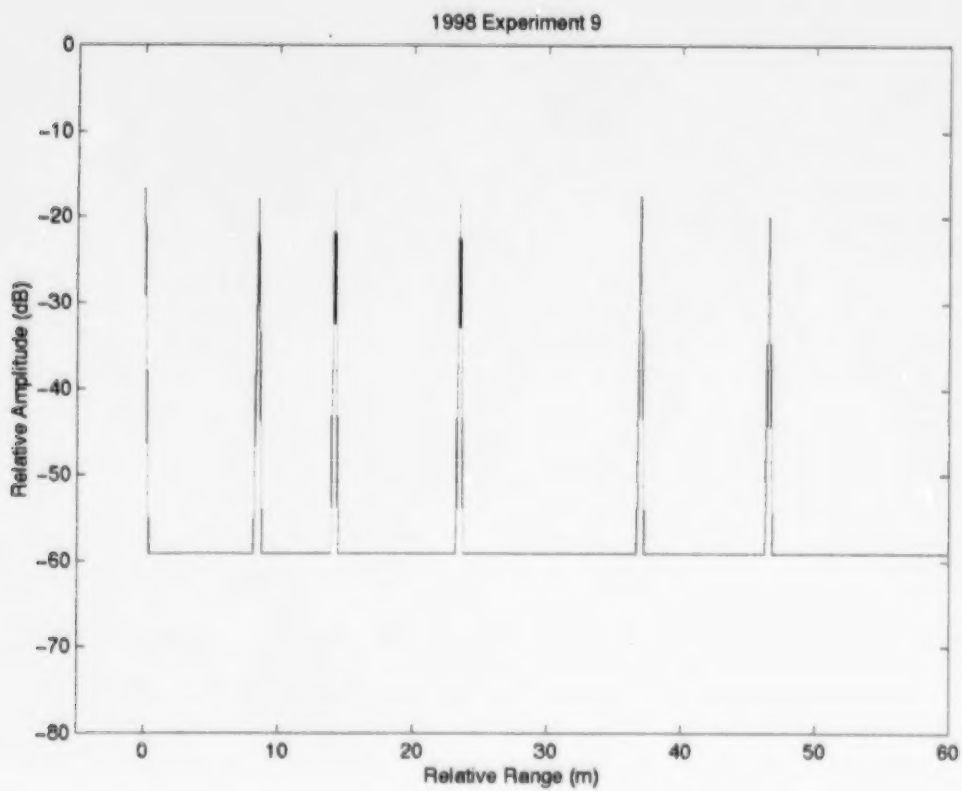
Figure 34: Overlapping Images for Measurement 9

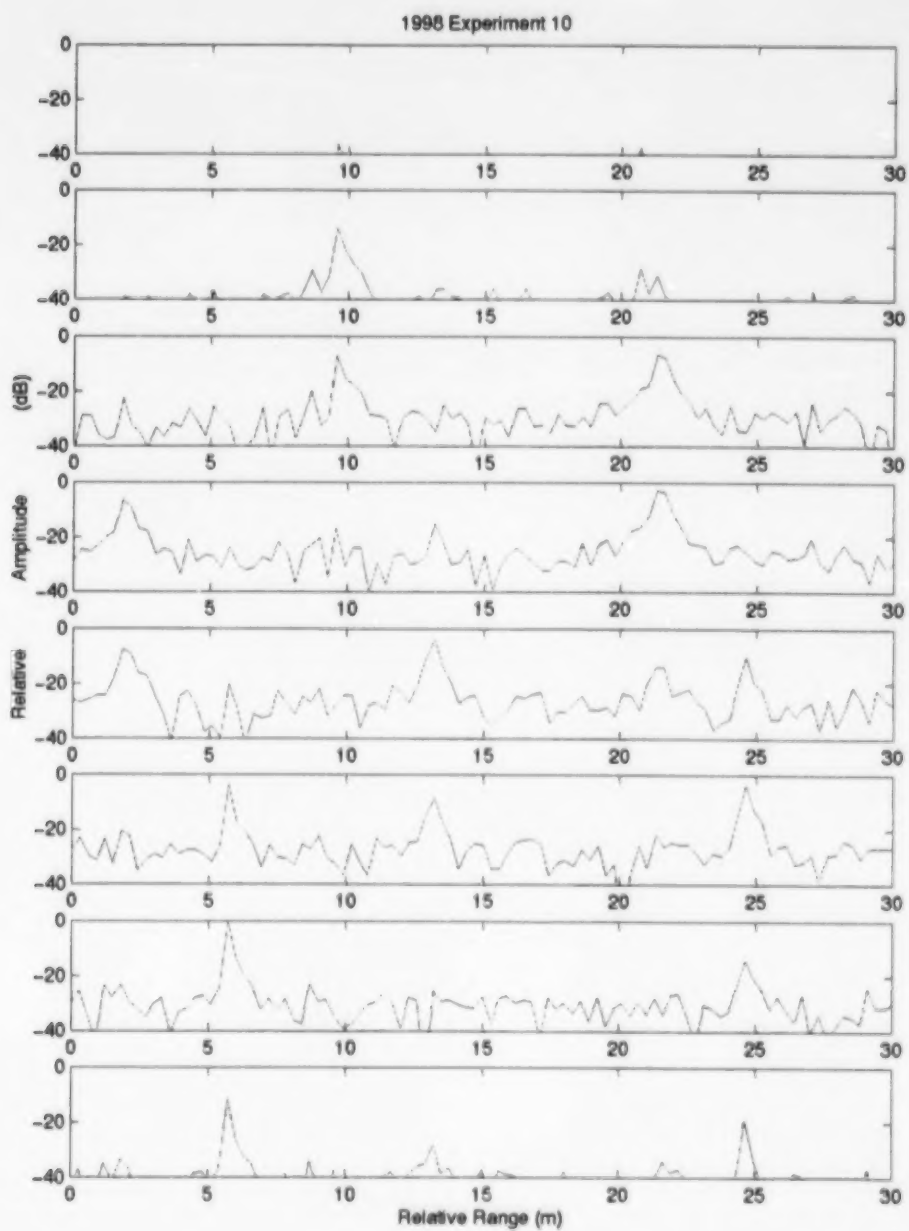**Figure 35: SPR Results for Measurement 9, Reflector Spacing 8, 6, 9, 13, 10 m**

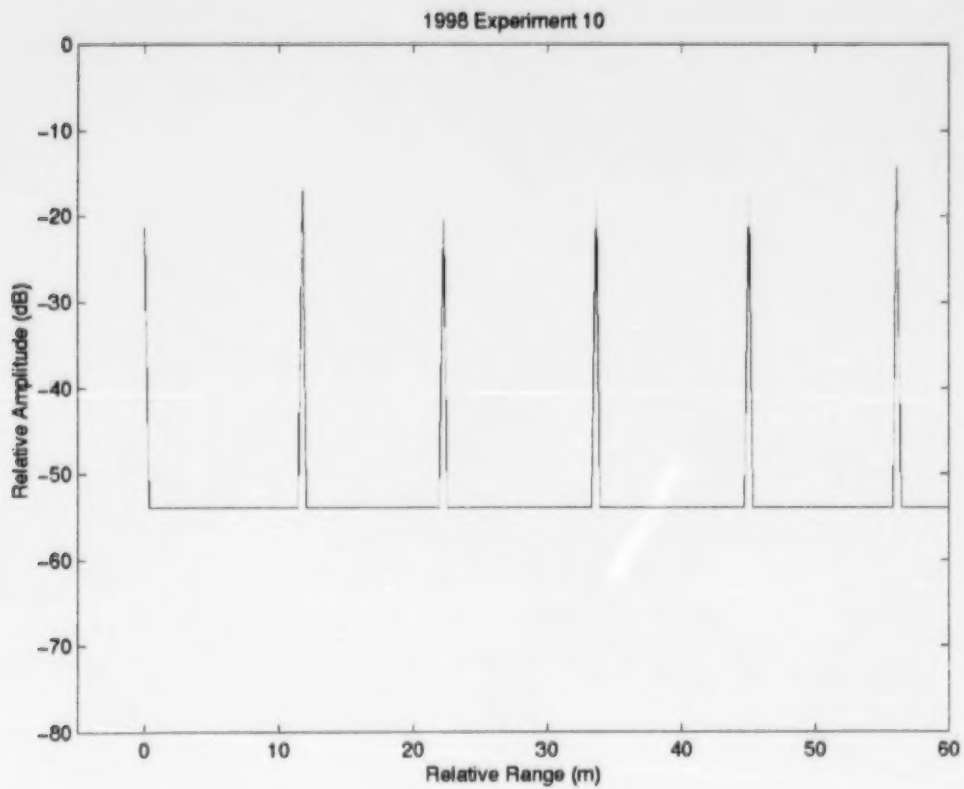Figure 36: Overlapping Images for Measurement 10.

Figure 37: SPR Results for Measurement 10, 6 Targets Evenly Spaced at 11 m Intervals

Table 7 displays the overall performance of the SPR routine for sorting out the reflectors. It was successful in determining all the reflector positions. A full reconstruction was not performed because of the multiple sidelobes and edge effect problems. The cause of this still needs to be investigated, as well as experiments on moving targets. EARS has been upgraded to have pulse to pulse frequency agility for further HRR studies.

	1998-7 Spacing (m)		1998-8 Spacing (m)		1998-9 Spacing (m)		1998-10 Spacing (m)	
	real	est.	real	est.	real	est.	real	est.
	4	3.75	9	9	8	8	11	11
	4	4.25	9	9	6	5.75	11	10.5
	11	11.25	9	8.75	9	9.25	11	11.25
			9	9.25	13	13.5	11	11.25
			9	9	10	9.5	11	11
Total	19	19.25	45	45	46	46	55	55

Table 7: Relative Peak Locations, Measured and SPR Estimates

8.0 CONCLUSIONS

Simulated studies for the SPR and SPI routines gave promising results. The studies tried to take into account imperfect compensation and SNR limitations. Inaccuracies in estimating the compensation requirements result in quite distorted HRR images. The identifiers only made use of the imperfect signatures, thus causing degradation in performance for the new and the conventional techniques. Additional preprocessing for "cleaning" the signatures would improve the results for all identifiers. Only errors for individual compensations were used to simplify the study. Both velocity and acceleration compensation errors gave rise to multiple peaks, or a defocusing of the HRR images. Velocity and acceleration tolerant waveforms [4] can be used to solve some of the compensation problems. The SPR routine performed better than the conventional HRR routine for compensation errors. The SPI routine didn't perform as well as the other techniques for the velocity compensation tests, however, it handled the acceleration offset tests better. If the compensation is perfect then the SPR and SPI routines perform as well as the conventional HRR process. As expected, they are more sensitive to SNR, but that is mainly due to only half the number of points being integrated as compared to the conventional HRR process. The SPR and SPI algorithms are designed for enhancing the radar's HRR capability, that is, they would be utilized when there is insufficient time to use the conventional stepped frequency waveform approach to identify an larger targets. The low resolution HRR worked better than all the other identifiers. This result highlights the problem of defining resolution requirements for HRR identification. The library generated for this study had targets containing up to 16 scatterers spread randomly across a 50 meter range. With this library, the identifiers may not need the 0.3 m resolution that the 500 MHz bandwidth gives to perform successfully. While the low resolution HRR approach worked better for this study, the SPR routine has demonstrated that it can be used to rebuild a target from multiple images, and also give good identification results. Determining a proper threshold is essential to the success of the SPR and SPI routines. The SPR sorting routine worked with experimental data of stationary targets. The SPR process has the advantage of increasing the maximum size of target that can be identified. It can also be used to give spacing between major scatterers. The experimental data also showed a potential pitfall for the SPR and SPI processes, namely the effect of range sidelobes.

Future studies will study the SPR technique using experimental radar data of moving targets. The Experimental Array Radar System has recently been upgraded so that data collection of moving targets is now possible. While it is possible to reduce dwell times by implementing the SPR or SPI process, the algorithms could also be used to enhance existing HRR systems by at least doubling the target size that could be identified.

9.0 ACKNOWLEDGEMENTS

10.0 REFERENCES

[1] "Coherent Radar Performance Estimation", James A. Scheer, James L. Kurtz Editors. Chapter 11, Artech House Incorporated, 1993.

[2] "Data Analysis A Bayesian Tutorial", D. S. Sivia, Oxford University Press, New York, March 1996.

[3] "Pattern Classification and Scene Analysis", R. O. Duda, P. E. Hart, Wiley-Interscience Publication, 1973.

[4] "Aircraft Recognition with Radar Range Profiles", R. Van Der Heiden, PHd thesis, University of Amsterdam, 1998.

SECURITY CLASSIFICATION OF FORM
(highest classification of Title, Abstract, Keywords)

DOCUMENT CONTROL DATA

(Security classification of title, body of abstract and indexing annotation must be entered when the overall document is classified)

1. ORIGINATOR (the name and address of the organization preparing the document. Organizations for whom the document was prepared, e.g. Establishment sponsoring a contractor's report, or tasking agency, are entered in section 8.)	2. SECURITY CLASSIFICATION (overall security classification of the document. including special warning terms if applicable)
Defence Research Establishment Ottawa 3701 Carling Avenue Ottawa, Ontario, K1A-0Z4	UNCLASSIFIED

3. TITLE (the complete document title as indicated on the title page. Its classification should be indicated by the appropriate abbreviation (S,C or U) in parentheses after the title.)

New Stepped Frequency Algorithms for High Range Resolution Radar: Short Pulse Reconstruction and Short Pulse Identification (U)

4. AUTHORS (Last name, first name, middle initial)

Riseborough, Edwin S.

Wilkinson, Anna

5. DATE OF PUBLICATION (month and year of publication of document)	6a. NO. OF PAGES (total containing information. Include Annexes, Appendices, etc.)	6b. NO. OF REFS (total cited in document)
February 2000	67	4

7. DESCRIPTIVE NOTES (the category of the document, e.g. technical report, technical note or memorandum. If appropriate, enter the type of report, e.g. interim, progress, summary, annual or final. Give the inclusive dates when a specific reporting period is covered.)

Technical Report

8. SPONSORING ACTIVITY (the name of the department project office or laboratory sponsoring the research and development. Include the address.)

DND - Defence Research Establishment Ottawa
3701 Carling Avenue
Ottawa, Ontario, K1A-0Z4

9a. PROJECT OR GRANT NO. (if appropriate, the applicable research and development project or grant number under which the document was written. Please specify whether project or grant)	9b. CONTRACT NO. (if appropriate, the applicable number under which the document was written)
1AA14	

10a. ORIGINATOR'S DOCUMENT NUMBER (the official document number by which the document is identified by the originating activity. This number must be unique to this document.)	10b. OTHER DOCUMENT NOS. (Any other numbers which may be assigned this document either by the originator or by the sponsor)
DREO TECHNICAL REPORT 2000-011	

11. DOCUMENT AVAILABILITY (any limitations on further dissemination of the document, other than those imposed by security classification)

(X) Unlimited distribution
( ) Distribution limited to defence departments and defence contractors; further distribution only as approved
( ) Distribution limited to defence departments and Canadian defence contractors; further distribution only as approved
( ) Distribution limited to government departments and agencies; further distribution only as approved
( ) Distribution limited to defence departments; further distribution only as approved
( ) Other (please specify):

12. DOCUMENT ANNOUNCEMENT (any limitation to the bibliographic announcement of this document. This will normally correspond to the Document Availability (11). However, where further distribution (beyond the audience specified in 11) is possible, a wider announcement audience may be selected.)

Unlimited

13. ABSTRACT (a brief and factual summary of the document. It may also appear elsewhere in the body of the document itself. It is highly desirable that the abstract of classified documents be unclassified. Each paragraph of the abstract shall begin with an indication of the security classification of the information in the paragraph (unless the document itself is unclassified) represented as (S). (C). or (U). It is not necessary to include here abstracts in both official languages unless the text is bilingual).

One of the problems facing Multi-Function Radar (MFR) designers is a limited time budget. Since an MFR has to perform many functions in parallel, time consuming functions, such as high range resolution radar (HRR), face time constraints which gravely limit their capability. MFR's under development are planning to use the stepped frequency waveform to implement HRR since it is a relatively simple waveform to implement, however, this requires the radar to dwell on the target for a long time. This report describes two new relatively simple techniques, called the short pulse reconstruction (SPR) technique and the short pulse identification (SPI) technique, which can be used to reduce the dwell time required for HRR. The new techniques presented here use a smaller pulse width to sample portions of the target, and would make use of high-speed analog-to-digital data acquisition systems that should already be part of an MFR. The SPR technique can create the complete target high range resolution amplitude versus range profile (or HRR image) based on returns from overlapping HRR images. The SPI technique is also presented, which performs identification directly using adjacent HRR returns. Simulated studies for the SPR and SPI routines gave promising results. If the compensation is perfect then the SPR and SPI routines perform as well as the conventional HRR process. Inaccuracies in estimating the compensation requirements resulted in quite distorted HRR images. The identifiers only made use of the imperfect signatures, thus causing a degradation in performance. However, the conventional HRR approach did not perform as well for most compensation errors. Since, at most, only half the frequencies are required by the SPR and SPI algorithms as that of the conventional HRR, the techniques are more sensitive to SNR. The SPR sorting routine was able to determine the geometry and relative signal strengths of various experimental configurations using an Experimental Array Radar System. While it is possible to reduce radar dwell times by implementing the SPR or SPI processes, the algorithms could also be used to enhance existing HRR systems by at least doubling the size of target they could identify.

14. KEYWORDS, DESCRIPTORS or IDENTIFIERS (technically meaningful terms or short phrases that characterize a document and could be helpful in cataloguing the document. They should be selected so that no security classification is required. Identifiers such as equipment model designation, trade name, military project code name, geographic location may also be included. If possible keywords should be selected from a published thesaurus. e.g. Thesaurus of Engineering and Scientific Terms (TEST) and that thesaurus-identified. If it is not possible to select indexing terms which are Unclassified, the classification of each should be indicated as with the title.)

Multi-Function Radar
High Range Resolution
Stepped Frequency Waveform
Non-Cooperative Target Recognition